AD-A063 929 ITEK CORP LEXINGTON MASS OPTICAL SYSTEMS DIV F/G 17/9
HYBRID OPTICAL/ELECTRONIC PROCESSOR STUDY.(U)
DEC 78 B A HORWITZ DAAG29-77-C-0027
UNCLASSIFIED PFR-78-105 NL

| OF |
AD
A063929

END
DATE
FILMED
3-79
DDC

ARO 15216.2-P

LEVEL II

12

SC

Report DAAG29-77-C-0027-Phase II

HYBRID OPTICAL/ELECTRONIC PROCESSOR STUDY

FINAL REPORT
DECEMBER 1978

Prepared by
ITEK CORPORATION
OPTICAL SYSTEMS DIVISION
10 MAGUIRE ROAD
LEXINGTON, MASSACHUSETTS 02173

UNDER CONTRACT: DAAG29-77-C-0027
DATE OF CONTRACT: JULY 1978

PF

Principal Investigator: Dr. Bruce A. Horwitz

Prepared for
U.S. Army Research Office
Box 12211
Research Triangle Park, North Carolina 27709

Prepared as a Laboratory Director's Project
for the Rome Air Development Center

79 01 17 008

Report DAAG29-77-C-0027-Phase II

HYBRID OPTICAL/ELECTRONIC PROCESSOR STUDY.

FINAL REPORT,
DECEMBER 1978

64 p.

Prepared by
ITEK CORPORATION
OPTICAL SYSTEMS DIVISION
10 MAGUIRE ROAD
LEXINGTON, MASSACHUSETTS 02173

UNDER CONTRACT: DAAG29-77-C-0027
DATE OF CONTRACT: JULY 1978

PFR-78-195

Principal Investigator: Dr. Bruce A. Horwitz

Prepared for
U.S. Army Research Office
Box 12211
Research Triangle Park, North Carolina 27709

Prepared as a Laboratory Director's Project
for the Rome Air Development Center

UNCLASSIFIED

SECURITY CLASSIFICATION OF THIS PAGE *(When Data Entered)*

REPORT DOCUMENTATION PAGE		READ INSTRUCTIONS BEFORE COMPLETING FORM
1. REPORT NUMBER DAAG29-77-C-0027 Phase II	2. GOVT ACCESSION NO.	3. RECIPIENT'S CATALOG NUMBER
4. TITLE *(and Subtitle)* HYBRID OPTICAL/ELECTRONIC PROCESSOR STUDY		5. TYPE OF REPORT & PERIOD COVERED Final Report
		6. PERFORMING ORG. REPORT NUMBER PFR 78-105
7. AUTHOR(s) Dr. Bruce A. Horwitz		8. CONTRACT OR GRANT NUMBER(s) DAAG29-77-C-0027
9. PERFORMING ORGANIZATION NAME AND ADDRESS Itek Corporation 10 Maquire Road Lexington, Massachusetts 02173		10. PROGRAM ELEMENT, PROJECT, TASK AREA & WORK UNIT NUMBERS
11. CONTROLLING OFFICE NAME AND ADDRESS U.S. Army Research Office Box 12211 Research Triangle Park, North Carolina 27709		12. REPORT DATE December 1978
		13. NUMBER OF PAGES
14. MONITORING AGENCY NAME & ADDRESS *(if different from Controlling Office)*		15. SECURITY CLASS. *(of this report)* Unclassified
		15a. DECLASSIFICATION/DOWNGRADING SCHEDULE

16. DISTRIBUTION STATEMENT *(of this Report)*

This document has been approved for public release and sale; its distribution is unlimited.

17. DISTRIBUTION STATEMENT *(of the abstract entered in Block 20, if different from Report)*

18. SUPPLEMENTARY NOTES

19. KEY WORDS *(Continue on reverse side if necessary and identify by block number)*

Hybrid processing, optical processing, radar imaging

HR cubed

20. ABSTRACT *(Continue on reverse side if necessary and identify by block number)*

Itek Corporation has performed a three-part study that addresses the use of hybrid optical/electronic processing techniques for high range resolution imaging radar systems. The first part of the study was an investigation of the processing requirements of the HR^3 system. Parametric evaluations were performed that related processor capabilities such as number of parallel processing channels to the basic system operating parameters such as cross-range resolution, target density, target range, and target velocity. → next page

DD FORM 1 JAN 73 1473 EDITION OF 1 NOV 65 IS OBSOLETE

UNCLASSIFIED

SECURITY CLASSIFICATION OF THIS PAGE *(When Data Entered)*

20. ABSTRACT (continued)

The second part of this study included a survey of hybrid processing systems that have already been assembled. This survey covered illustrative examples of the different types of hybrid processors, including power spectrum analyzers, Fourier transform filtering systems and synthetic aperture radar processors.

The third part of this study developed a strawman hybrid processor for HR^3 image generation. In keeping with hybrid design philosophy, the system included optical subsystems for pulse compression, mass storage, Fourier transformation, and image correlation.

The conclusions of this study were: (1) There is a particularly strong need for the high throughput rates of hybrid techniques in the "front end" portions of the processor. (2) There already exist hybrid systems that match or nearly match some of the processing tasks that occur in HR^3 imaging. Specifically, hybrid pulse compressors and one-dimensional real-time Fourier transformers. (3) There exists a significant need for continuing research efforts in terms of both the hybrid systems as applied to the HR^3 application and the HR^3 algorithms themselves.

ABSTRACT

Itek Corporation has performed a three-part study that addresses the use of hybrid optical/electronic processing techniques for high range resolution imaging radar systems. The first part of the study was an investigation of the processing requirements of the HR^3 system. Parametric evaluations were performed that related processor capabilities such as number of parallel processing channels to the basic system operating parameters such as cross-range resolution,target density, target range, and target velocity.

The second part of this study included a survey of hybrid processing systems that have already been assembled. This survey covered illustrative examples of the different types of hybrid processors, including power spectrum analyzers, Fourier transform filtering systems and synthetic aperture radar processors.

The third part of this study developed a strawman hybrid processor for HR^3 image generation. In keeping with hybrid design philosophy, the system included optical subsystems for pulse compression, mass storage, Fourier transformation, and image correlation .

The conclusions of this study were: (1) There is a particularly strong need for the high throughput rates of hybrid techniques in the "front end" portions of the processor. (2) There already exist hybrid systems that match or nearly match some of the processing tasks that occur in HR^3 imaging. Specifically, hybrid pulse compressors and one-dimensional real-time Fourier transformers. (3) There exists a significant need for continuing research efforts in terms of both the hybrid systems as applied to the HR^3 application and the HR^3 algorithms themselves.

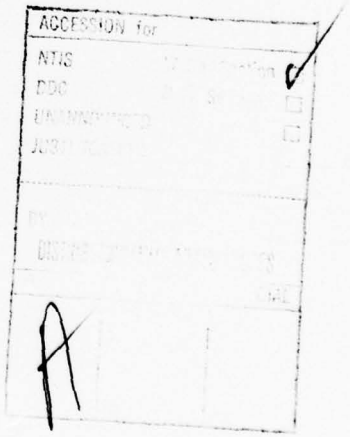

CONTENTS

FIGURES

TABLES

1. INTRODUCTION

The data burden for noncooperative target identification friend or foe (IFF) systems has increased dramatically over the days of the binocular-equipped spotter. The high speeds and weapon ranges of target aircraft have enlarged the region in which target identifications must be made, and the long range sensors that have been developed do not individually provide sufficient data on which to base the friend or foe decision. Therefore, data from several types of sensors must be processed together to increase the IFF confidence level. This combination of multisensor, multiple target processing has outstripped the capabilities of reasonably sized, digital processing systems.

An alternative to purely digital processing is hybrid optical/electronic processing in which the unique advantages of optical and digital processors are combined with proper design, so as to be complementary. Digital systems bring flexibility, quantitative accuracy, and Boolean logic to the marriage, while analog optical systems provide two-dimensional, speed-of-light, parallel multiplications, Fourier transforms, and correlations. For example, high range resolution radar (HR^3) returns, if raster recorded, could be optically pulse-compressed and pseudo-Doppler processed instantaneously to form a two-dimensional "image" of the target. The mensuration of this image could then be carried out electronically since a digital computer could correct for aspect angle, direction of flight, and other parameters measured by the tracking radars.

Optimum performance of the total hybrid system depends critically on proper design and balance in the assignment of processing tasks between the digital and analog subsystems. In order to better understand the tradeoffs involved, the Rome Air Development Center has begun to study how and where hybrid techniques might be utilized. Itek Corporation has undertaken the Hybrid Optical/Electronic Processing Study with three primary goals: (1) study the IFF processing requirements, with particular emphasis on the HR^3 sensor, to create a basis for hybrid system design, (2) conduct a literature search to define the state of the art in hybrid processing, and (3) provide a baseline system configuration of a hybrid optical/electronic processor for consideration and analysis and to provide a focus for further investigations.

This report is divided into sections that follow along the lines of the three goals outlined above. Naturally, there has been some interaction between the three phases of the study so that a coherent evaluation of hybrid techniques has resulted. Because of the constraints of time and the charter of the sponsor, Itek has concentrated its efforts on the HR^3 imaging sensor, to the exclusion of all others. As discussed in Section 2, this division falls along a natural boundary, but the utility of hybrid techniques may very well cross this boundary. Section 3 of this report surveys existing hybrid processors. The systems included in this survey are intended to be representative rather than inclusive since many variations on each system are possible. Section 4 presents a hybrid system for IFF processing that incorporates features of previously designed subsystems. Section 5 is a summary that includes Itek's conclusions and recommendations for further efforts.

2. AIRCRAFT IDENTIFICATION WITH WIDEBAND COHERENT RADARS

2.1 INTRODUCTION

It is an understatement to say that in modern tactical air warfare scenarios the identification of possible targets as friends or foes has become increasingly difficult. Because of the stakes involved, the highest probability IFF system possible is required (fratricide is unacceptable). Even today, that system is direct visual confirmation. Unfortunately, as the speeds of targets and the ranges of weapons systems have increased, vision-based IFF systems have become increasingly less effective since a foe's standoff distance for firing may exceed the visual range. The situation becomes even more difficult when the next level of IFF processing (i.e., for command and control) is considered. In all likelihood, no system based on the data from a single sensor type will be able to provide the accuracy; in this type of scenario, the system most likely to succeed is the one that develops target signatures in as many bands as possible.

As shown in Fig. 2-1, the processing of multisensor data may be divided into three natural categories: signature generation, target classification, and target identification. Signature generation occurs when the raw data from an individual sensor is processed to extract the target related information. For example, the raw data returns from high range resolution radars must be "pulse compressed" to yield fine range data, while simultaneous measurement of the carrier phase can be processed to generate cross-range resolution as well. The distribution of pulses in range and cross-range positions is the signature of the target. One uniform characteristic of signature generation processing is that no logical operations are called for. No quantitative comparisons with stored data are required either, and exactly the same manipulations are applied to all incoming data. This is not true of target classification and identification processing.

In general, the difference between classification and identification is a matter of degree rather than of kind. In both types of processing logical operations are usually required, quantitative measurements may be used, and probabilistic decisions made. For the purposes of this paper, a classifier will be defined as a processor that operates on a single sensor signature in order to select one or more features of the target. The extracted feature can be either at a high level ("twin jet exhausts") or a lower level ("25 feet between wing tips"). It should be noted that a classifier may have several outputs, e.g., length, width, height.

An identifier is similar to a higher dimensional classifier; it places the target in a class based on country of origin (or, at least, friend or foe). The inputs to the identifier are the outputs of one or more classifiers. Some appropriate algorithm is then required to combine the very different types of classification elements (dimensions, exhaust temperatures, velocities, etc.) into an effective identification. This algorithm must also be able to assign a

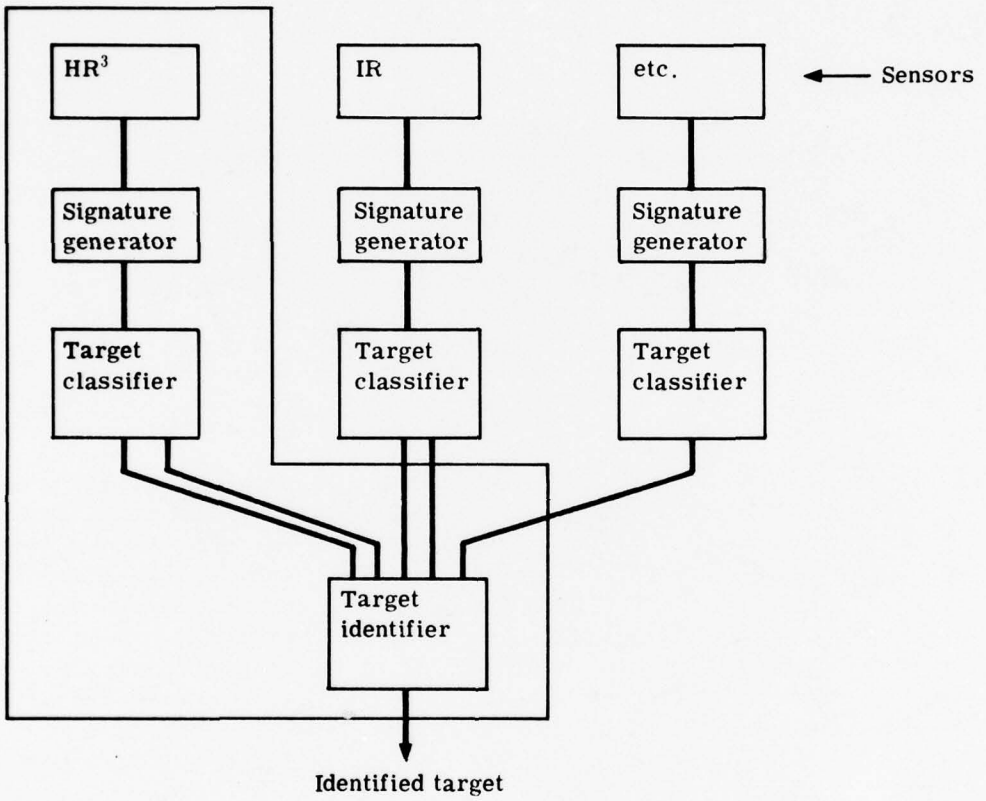

Fig. 2-1 — Multisensor IFF system block diagram

probability of error to its selection, based on some measure of "closeness" to a reference prototype for that target.

In reviewing the operations of the three stages of IFF processing, it becomes obvious that highly complex procedures are involved that would involve extremely large electronic data burdens. Some phases of the processing seem as if they could be handled more expediently, by a human eye-brain computer. (Humans make excellent inferential judgments.) Unfortunately, both electronic and human components have space/speed/cost limitations that make them less desirable in multiple-target, tactical situations. One possible means of increasing the throughput of an IFF system is to introduce optical/electronic hybrid processors at various locations in the system. In order to determine if hybrid techniques are even suitable for this application, Itek has studied the particular processing requirements of one sensor — the high range resolution radar. As indicated in Fig. 2-1, this concentration is quite natural from the structure of an IFF processing system; data from different sensors are not fused until late in the processing algorithm. Thus, this study leaves untouched the question of hybrid technique application to other sensor processing chains.

The HR^3 sensor was selected because of RADC's involvement with the sensor and because the feasibility of the method has already been demonstrated with radar returns from aircraft models in the laboratory and from real aircraft in the field.[1-4]* Emphasis is now being placed on the development of improved algorithms, solution of several radar hardware problems, and examination of new approaches to the signal and data processing.

In HR^3 systems, signature generation consists of processing the returned radar signals to generate images of the targets. Classification consists of extracting dimensional information and other features of the image to categorize the target in general terms. The final identification is accomplished by a detailed comparison of the features extracted from the image, with the corresponding features of known aircraft types within the categories identified in the classification task.

The total processing load strongly depends on the operational scenario. In particular, some of the most important variables that impact the total burden of the processor are the rate at which aircraft are input to the identification system, the aircraft velocities including their direction with respect to the radar line of sight, various radar parameters, the required resolutions and unambiguous windows, the algorithms used for the three processing tasks, and the time allowed for a decision to be made.

In this section, the processing required for aircraft identification using wideband, coherent radar imaging is examined. The algorithms for the three processing tasks are discussed in Sections 2.2, 2.3, and 2.4. Section 2.5 sets up a general scenario and analyzes the total burden placed on the processor.

2.2 SIGNATURE GENERATION

2.2.1 Imaging Algorithm

The algorithm for obtaining images of aircraft using wideband, coherent radar data is closely related to the algorithm used in synthetic-aperture radar systems.[5] Imaging in the slant range direction is accomplished with pulse compression techniques to obtain very high range resolution. Cross-range (azimuth) imaging is performed by Doppler processing of the coherent returned signal to obtain the components along the radar line of sight of the relative velocities of the various scatterers on the aircraft. The velocities are converted into cross-range coordinates by assuming the airplane is rotating with constant angular velocity with

*References are listed in Section 2.6

respect to the radar location. If the aircraft is not flying along the radar line of sight, there is a rotation present (even if the plane is not rotating about its own center of motion) due to the change in aspect angle between the radar line of sight and the target track as it travels.

There are two primary differences between aircraft imaging as discussed here and the imaging of terrain by synthetic-aperture techniques: (1) the object being imaged is much smaller and (2) the relative motion between target and radar can be variable, and is unknown. The first difference makes the aircraft imaging problem simpler since the geometrical corrections of the wavefront that are required in terrain mapping systems are not required. The second difference makes the aircraft imaging problem more difficult, however, because it is necessary to subtract from the returned data the motion of the center of rotation. Several approaches to this problem have been suggested by Syracuse Research Corporation [1,2] and by the University of Southern California Image Processing Institute.[3,4]

In order to obtain an understanding of the signal processing involved in obtaining a radar image, it is useful to consider the imaging problem as an inverse-scattering problem, i.e., the problem of obtaining the properties of the scatterers from a knowledge of the scattered radiation. If the signal transmitted by the radar is f(t), where t is time, then the returned signal is proportional to

$$s(t) = \iiint_V \rho(\underline{r}')\, f[t - 2R'(t)/c]\, d\underline{r}' \tag{1}$$

The Cartesian components of the vector $\underline{r}'$ are specified in terms of a Cartesian coordinate system that is fixed with respect to the target (see Fig. 2-2). As the target translates and rotates, so does the coordinate system. The vector $\underline{r}'$ is the vector from the origin of that coordinate system to a point on the target. Since the target is a rigid body, $\underline{r}'$ does not change with time. $\rho(\underline{r}')$ is the reflectivity of the target at the point $\underline{r}'$. $R'(t)$ is the magnitude of the vector $\underline{R}'(t)$ (referred to an inertial frame) from the radar to the point $\underline{r}'$. As the target moves, $\underline{R}'(t)$ changes with time. The relationship between $\underline{R}'(t)$ and $\underline{r}'$ is given by

$$\underline{R}'(t) = \underline{R}_0(t) + \underline{\underline{M}}(t) \cdot \underline{r}' \tag{2}$$

where $\underline{R}_0(t)$ is the vector (referred to an inertial frame) from the radar to the origin of the coordinate system fixed with the target and $\underline{\underline{M}}(t)$ is the dyadic that describes the rotation of the coordinate system about its origin. The integral in Eq. 1 extends over the target. The objective of the inverse-scattering problem is to determine $\rho(\underline{r}')$ from a knowledge of $s(t)$.

One approach to inverting Eq. 1 is to pass the received signal through a filter matched to the transmitted signal. This approach has the advantage of minimizing the effects of received noise.[6] The time shift introduced in the filter can be interpreted as a delay introduced by the round-trip propagation along a vector $\underline{R}(t)$ from the radar. Hence the output of the filter is given by

$$E(R) = \int_{-\infty}^{\infty} s(t)\, f^*[t - 2R(t)/c]\, dt \tag{3}$$

The imaging properties of this processing can be seen by substituting Eq. 1 into Eq. 3 and interchanging the order of integration to obtain

$$E(R) = \iiint_V \rho(\underline{r}')\, \chi(R' - R)\, dr' \tag{4}$$

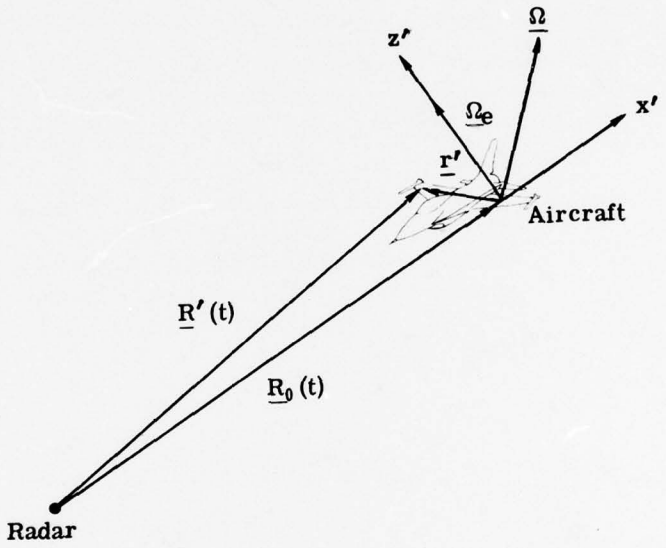

Fig. 2-2 — Coordinate system fixed with respect to the aircraft shown at time t_0

where $\chi(R' - R)$ is the ambiguity function $f(t)$.

Now, suppose that $\chi(R' - R)$ has a single sharply peaked maximum located at a point $\underline{r}' = \underline{r}$. Then it is clear from Eq. 4 that $E(R)$ will be an image of $\rho(\underline{r}')$. Indeed, if $\chi(R' - R) = \delta^3(\underline{r}' - \underline{r})$, then $E(R) = \rho(\underline{r})$ and a perfect image would be obtained.

The waveform of primary interest consists of a series of identical, equally spaced, nonoverlapping, modulated short pulses

$$f(t) = \sum_{n=-N/2}^{N/2} g(t - n\tau) \exp[i\omega_0 (t - n\tau)] \tag{5}$$

where ω_0 is the angular carrier frequency, $g(t)$ is the complex modulation function, τ is the spacing between pulses, and N is the total number of pulses. The pulses are taken to be short enough so that the motion of the target is negligible during the duration of the pulse.

The imaging algorithms that have been developed make use of the simplifying assumption that for the time interval of length $T = n\tau$, during which the target is irradiated by the waveform $f(t)$, the motion of the target with respect to the point $\underline{R}_0(t)$ can be taken to be a constant rotation specified by an angular velocity $\underline{\Omega}$.

It is then convenient to set up a Cartesian coordinate system (x', y', z') fixed in (and moving with) the target with origin at $\underline{R}_0(t)$. At the time $t_0 = R_0/c$, the x' axis lies along the vector $\underline{R}_0(t)$. The coordinate system at $t = t_0$ is illustrated in Fig. 2-2. As time progresses, the coordinate system rotates with the target away from the position shown. It is shown in the Appendix that with the point $\underline{r}'$ on the target referred to this coordinate system, the distance from the radar to that point is approximately

$$R'(t) \cong R_0(t) + x' + (t - t_0)\,\Omega_e\, y' \tag{6}$$

as long as the target rotates only a few degrees during the period of interest.

The imaging algorithm can be simplified further by replacing the ambiguity function in Eq. 4 with its absolute value to obtain

$$E'(R) = \iiint_V \rho(\underline{r}')\, |\chi(R' - R)|\, dr' \tag{7}$$

The important imaging properties of Eq. 7 are the same as those of Eq. 4.

It is shown in Appendix A that under the conditions being discussed, the magnitude of the ambiguity function is given by

$$|\chi(R' - R)| = \varphi(x' - x) \sum_{n=-N/2}^{N/2} \exp[-i\omega_0 2n\tau\, \Omega_e (y' - y)/c] \tag{8}$$

where $\varphi(x' - x)$, is the modulus of the autocorrelation of the modulation function $g(t)$.

Since the operations required to calculate $|\chi(R' - R)|$ as given in Eq. 8 separate into distinct operations for the x and y directions, the processing becomes quite simple. The received signal is correlated with the modulation function $g^*\{t - 2[R_0(t) + x]\}$ to perform the imaging in the x' direction and is Fourier transformed [by multiplying the n-th pulse by $\exp(i\omega_0 2n\tau\, \Omega_e y/c)$ and summing all pulses] to perform the imaging in the y' direction.

Note that a knowledge of $R_0(t)$ and Ω_e are required to perform the imaging. The most convenient way to handle the motion of the center of rotation $R_0(t)$ is to subtract the time delay $-2R_0(t)/c$ from the received data so that it does not have to be included in the matched filter.

2.2.2 Image Properties

The properties of the image are determined by the magnitude of the ambiguity function, which in turn depends on the transmitted waveform being used. The transmitted pulse of primary interest is the linear frequency-modulated (chirped) pulse given by

$$g(t) = \exp(i\alpha t^2) \qquad \text{for} \qquad |t| \leq \tau_0 \tag{9a}$$

$$g(t) = 0 \qquad \text{for} \qquad |t| > \tau_0 \tag{9b}$$

It is shown in reference 5 that with this modulation function, the magnitude of the ambiguity function given in Eq. 8 becomes

$$|\chi(R'-R)| = \left| \frac{\sin[2\alpha\tau_0(x'-x)/c]}{2\alpha(x'-x)/c} \quad \frac{\sin[(N+1)\omega_0\tau\Omega_e(y'-y)/c]}{\sin[\omega_0\tau\Omega_e(y'-y)/c]} \right| \tag{10}$$

The important properties of the image can be obtained from Eq. 10. It follows from Eq. 7 that the image in (x, y, z) space of a single point at (x′, y′, z′) on the target is given by the modulus of the ambiguity function. Consider the image of a point (x′, y′, z′). It is seen from the first quotient in Eq. 10 that the image varies in the range (x) direction as a sinc function with its peak at $x = x'$. As is well known, this factor attains a value 3 dB down from its maximum value when the argument of the sine function is about 1.4. The range resolution δ_R is equal to twice the value of $|x'-x|$ that is obtained by setting the argument of the sine term equal to this value. Hence, the range resolution obtained when a linear frequency modulated pulse is used is

$$\delta_R = 1.4c/\alpha\tau_0 \tag{11}$$

The properties of the image in the cross-range direction follow from the properties of the second quotient in Eq. 10. That factor has a series of equally strong peaks located wherever the argument of the sine function in the numerator is equal to an integral multiple of π. Hence, there are images at

$$y = y' + \frac{M\pi c}{\omega_0\tau\Omega_e} \tag{12}$$

for all integral M. Consequently, there is an image at $y = y'$ as desired, but there are additional images that must be eliminated by appropriate restriction of the field of view in order to avoid ambiguities.

The cross-range azimuth resolution is determined by the width of the peaks of the second quotient in Eq. 10. Just as in the case of range resolution, the cross-range resolution δ_{CR} is equal to twice the value of $|y-y'|$ that is obtained by setting the argument of the sine term in the numerator equal to 1.4. Hence, the azimuth resolution is given by

$$\delta_{CR} = 2.8c/[(N+1)\omega_0\tau\Omega_e] \tag{13}$$

Finally, since the ambiguity function is independent of z and z′, it is seen that the processing does not provide any imaging in the z′ direction. According to Eq. 7, the reflectivity of the target is simply integrated in the z′ direction in the final processed signal.

2.3 CLASSIFICATION

Once the image of the aircraft is generated, the processing required for identifying the aircraft can begin. The purpose of the classification task is to reduce the number of variables that must be considered to perform the identification. For example, in the approach suggested by SRC[2], aircraft dimensional information and other properties of the image are determined and used to place the unknown aircraft in one or more categories. Then, the identification task need consider only aircraft within those categories as possibilities.

In more general terms, this task consists of extracting a number of features of the image to be used for identification. The features that are most appropriate for final identification are highly dependent on the properties of the objects to be identified, the nature of sensors used, the characteristics of the imagery, and the approach used in the identification task. They must be chosen carefully so that nonrelevant data is ignored without losing information that is useful for identification. At present, there are no generally applicable techniques for determining the optimum features to be used. Methods are ad hoc, being highly dependent on the problem at hand.

In principle, features of the radar return signal could be extracted directly without performing the imaging. Such features are not very applicable to identification, however, since it would be necessary to measure and store the radar signatures from all possible targets at many different aspects. It would be very difficult to obtain the required data, especially for enemy aircraft. Moreover, the number of features required would make the process prohibitive.

By converting the radar returns to aircraft images, it becomes possible to employ features already known for all aircraft from photographs, etc. Moreover, changes in aircraft aspect can usually be taken into account mathematically so that data for known aircraft is needed at only a few aspect angles.

Because there is such a small HR[3] image data base, it is very difficult to tell what features will provide maximum discrimination. It is reasonable to expect that certain quantitative features — wing span, length, etc. — will be useful discriminators. In addition, qualitative features such as wing shape or tail shape seem to be likely candidates for discriminators. However, until the data base is established, it is almost impossible to tell whether these qualitative features will be extractable from the radar images.

2.4 IDENTIFICATION

The final task in the IFF process is to identify the target from the features extracted during the classification task. It is at this stage of the processing that data from parallel sensor channels is combined. Within the identification processor, all features are stripped of their connotative meanings: the processor does not care that the target seems to have delta wings, rather it cares that there is a p percent confidence that the target has feature f_1. In this way, all types of features (HR[3], IR, JEM, etc.) can be combined without the problem of how to compare "apples and oranges."

The most difficult aspect of target identification is the development of the identification algorithm. This algorithm may be extremely simple, such as identifying the target using only the feature that has the highest probability of being correct, or, more likely, it will be a complex weighting of all features. One approach would be to metrify (e.g., put on a 1 to 10 scale) all features and use these metrics as vector components in an M-dimensional space. The Euclidian

distance between a target's vector and a known reference vector is used as the measure of likelihood that the target is the same as the reference. Another approach is to develop a discriptor function that weights each feature for each known reference. When the target feature values are used in the discriptor functions, the function that has the largest value indicates the target's identification. A more complicated iterative approach is to vary the weights of the features depending on the preliminary subset of possible identifications. That is, if the first pass limits the possible identification to two references, both of which are known to have the wing shape, then wing shape is given zero weighting on the second iteration.

The identification processor can be used in a loop with the feature extraction processor in order to reduce the processing load. If, for example, a correlation process is used to extract qualitative features from images, then data from the identifier (and the tracking radar) can be used to limit the list of reference features to try in the correlator. If the tracking radar indicates that the target is heading cross-range, then the correlator need not try to match head-on views.

2.5 PROCESSOR REQUIREMENTS

In a conflict situation, it will be necessary to identify a large number of aircraft in as short a time as possible. In order to estimate the burden placed on the imaging processor, it is sufficient to apply a very simple scenario. Suppose the planes are uniformly distributed in space and are all flying in straight horizontal lines with the same speed, V, uniformly distributed in direction. Let P be the integral over all altitudes of the number of planes per unit volume traveling into a unit angle. Suppose also that the radar has a maximum range Q and a semicircular field of view (see Fig. 2-3). Assume that the aircraft that enter the field of view from behind the radar (and hence are traveling away from the radar) do not need to be processed.

2.5.1 Number of Parallel Channels

The number of parallel channels that are required within the radar image processor may be determined by considering the processor as a pipeline into which data from acquired planes is fed, and out of which images of planes are received. The number of planes in the pipeline on an average depends on the rate at which planes are acquired and the length of time required for processing each plane. The processor must contain one channel for each plane in the pipeline. If we assume that the radar imaging is performed in a hybrid processor, then the processing time per plane is essentially equal to the theoretical integration time, T, required by the algorithm to achieve a given cross-range resolution. Since the integration time is a function of the aspect angle, the number of planes in the pipeline due to each aspect angle must be calculated first, and that result integrated over all angles.

The relationship between the radar parameters and the integration time is given by Eq. 13. Since $N + 1 \cong N$ for large N and since $T = N\tau$, Eq. 13 can be rewritten as

$$T \cong 2.8\, c/\delta_{CR}\, \omega_0\, \Omega_e \tag{14}$$

Because the aircraft are flying in straight lines, the angular velocity of the aircraft at maximum range Q is given by

$$\Omega_e = V \sin \eta/Q \tag{15}$$

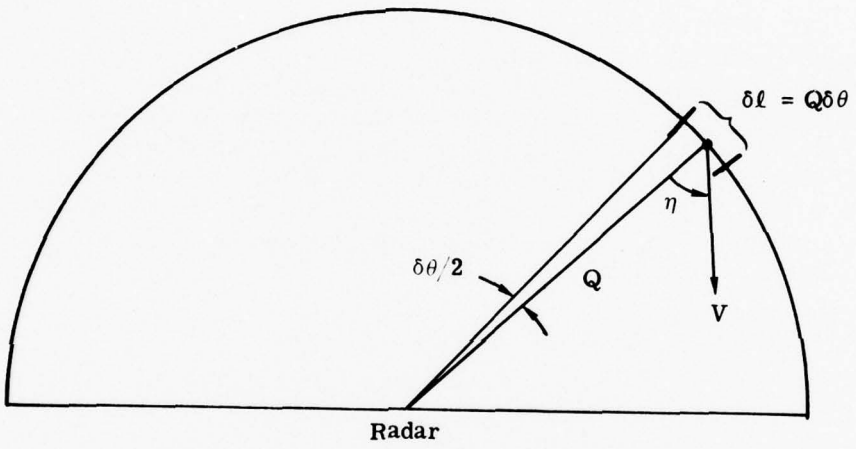

Fig. 2-3 — Field of view of the radar

where η is the aspect angle between the flight path and the radar line of sight. Hence, if the aircraft range does not change much during T, Eq. 14 becomes

$$T \cong 1.4\lambda R/\pi\, \delta_{CR}\, V \sin \eta \tag{16}$$

where λ is the radar wavelength.

Since Eq. 16 is the integration time required for a plane flying at the angle η, the rate at which planes enter the field of view from that angle, P_η, must now be calculated. P_η can be related to the aircraft density P as follows. At any point on the semicircle of radius Q, shown in Fig. 2-3, the number of planes traveling into the semicircle with aspect angle η per unit angle in a unit time is

$$\delta P_\eta = P\, V\, \delta l \cos \eta \tag{17}$$

where

$$\delta l = Q \delta \Theta \tag{18}$$

is an element of arc along the semicircle. Since all quantities are independent of Θ, Eq. 17 and Eq. 18 integrated over the semicircle give

$$P_\eta = \pi\ P\, V\, Q \cos \eta \tag{19}$$

The multiplication of Eq. 16 and Eq. 19 gives the final expression for the total number of aircraft with aspect angle η per unit angle that are being processed simultaneously:

$$N_\eta = 1.4\lambda\, Q^2\, P \cot \eta / \delta_{CR} \tag{20}$$

Since $N\eta$ grows without limit as η approaches 0, it is not feasible to generate images of aircraft with aspect angle too close to zero. Hence, the aircraft returns that are processed are those with aspect angles η such that $-\pi/2 \le \eta \le -\eta_0$ or $\eta_0 \le \eta \le \pi/2$, where η_0 is a positive cutoff angle. If η_0 is large enough so that the range of all aircraft being processed remains nearly equal to Q during the processing time, then the total number of planes that must be processed simultaneously is given by

$$N_P = 2\int_{\eta_0}^{\pi/2} N_\eta\, d\eta = \frac{2.8\lambda Q^2\, P \ln\left(\frac{1}{\sin \eta_0}\right)}{\delta_{CR}} \tag{21}$$

Eq. 21 is the expression for the total number of parallel channels required under the assumed conditions.

2.5.2 Data Rate

The average pulse repetition frequency, F, that is required to obtain a desired unambiguous cross-range window, W_{CR}, for all targets is determined by Eq. 15 in terms of the radar and aircraft parameters. Setting $W_{CR} = y - y'$ and $m = 1$ and substituting Eq. 18 into Eq. 15 yields

$$W_{CR} = Q\lambda/2\, V \tau \sin \eta \tag{22}$$

Since the pulse repetition frequency is $1/\tau$, the rate that pulses must be processed for each aircraft with aspect angle η is

$$f_\eta = \frac{1}{\tau_\eta} = \frac{2 W_{CR} V \sin \eta}{Q\lambda} \tag{23}$$

Eq. 23 gives the data rate required for the cross-range processing for each channel. Each pulse provides one sample in the discrete Fourier-transform relation in Eq. 9 that is applied to perform the cross-range imaging. It follows from Eq. 23 that the aircraft with larger aspect angle require higher data rates. The pulse repetition frequency, F_η, for all aircraft with the same aspect angle is the product of the number of planes at that angle, Eq. 20, and the pulse repetition frequency for that angle, Eq. 23:

$$F_\eta = N_\eta f_\eta = 2.8 Q P W_{CR} V \cos \eta / \delta_{CR} \tag{24}$$

Hence, the data rate for all aircraft with the same aspect angle taken together decreases with aspect angle η.

The total number of outgoing pulses per second that must be produced for all channels taken together is the integral of Eq. 24 taken over all aspect angles:

$$F = 2 \int_{\eta_0}^{\pi/2} F_\eta \, d_\eta = 5.6 Q P W_{CR} V (1 - \sin \eta_0)/\delta_{CR} \tag{25}$$

2.5.3 Number of Correlators and Fourier Transformers

When the image processor is considered as a pipeline, with acquired targets entering one end and images exiting at the other end, it becomes obvious that the rate at which Fourier transforms must be produced is equal to the rate of exiting images. (After all, one Fourier transform is required for each image.) The rate at which targets enter the processing pipeline is calculated by integrating P_η over the angular field of interest. Integrating Eq. 19 over the range $\eta_0 \leq \eta \leq \pi/2$ and $-\eta_0 \geq \eta \geq -\pi/2$ yields the rate of Fourier transforms

$$R_T = 2\pi \ P V Q \ (1 - \sin \eta_0) \tag{26}$$

If t_T seconds are required to perform each transformation, then the number of Fourier transform processors required is

$$N_T = R_T t_T = 2\pi \ P V Q t_T \ (1 - \sin \eta_0) \tag{27}$$

A similar calculation may be made to determine the number of correlators required. However, in this case the limiting factor is less likely to be the correlation speed per se, but rather the desired unambiguous range window. In order to achieve an unambiguous range window, W_R, each outgoing pulse will produce a string of return pulses spread over a time

$$t_c = W_R/c \tag{28}$$

Return pulses from a different outgoing pulse must be processed in an additional correlator if the two outgoing pulses were any closer than t_c. (Note: It is assumed that all targets are at essentially the same range and that returns from different outgoing pulses can be separated because they are on different formed beams in a phased array.) The minimum number of

correlators is then the product of Eq. 25 and Eq. 28:

$$N_c = Ft_c = 5.6\ PQV W_{CR}\ W_R\ (1 - \sin \eta_0)/\delta_{CR}. \tag{29}$$

2.5.4 Evaluation of η_0

All of the results derived above depend on the parameter η_0, the minimum aspect angle processed. It is obvious that there is some nonzero minimum value for η_0 because at zero (i.e., boresight) there is no apparent target rotation. However, the limiting factor on η_0 turns out to be the algorithmic assumption of constant angular rotation. If the plane travels too far during the integration time, the image will be smeared because Ω_e does not remain constant. When the temporal Fourier transform is taken to perform the cross-range imaging, the Fourier-transform variable ω' is related to the cross-range location y by

$$\omega' = \frac{2\omega}{c}\ \Omega_e\, y \tag{30}$$

Hence, if Ω_e is off by an amount $\Delta\,\Omega_e$, the image location is off by an amount $\Delta\, y$ given by

$$\Delta\, y = \frac{y}{\Omega_e}\ \Delta\,\Omega_e \tag{31}$$

If Ω_e changes by an amount $\Delta\,\Omega_e$ as the plane travels, the image is smeared over an amount $\Delta\, y$. If $\Delta\, y$ is to be less than the resolution, then $\Delta\,\Omega_e$ must satisfy

$$\Delta\,\Omega_e \leq \Omega_e\ \delta_{CR}/y \tag{32}$$

The largest possible value of y is $W_{CR}/2$. Hence,

$$\Delta\,\Omega_e \leq 2\,\Omega_e\,\delta_{CR}/W_{CR} \tag{33}$$

Since Ω_e is related to the aircraft flight path by

$$\Omega_e\,(t) = V \sin \eta\,(t)/r\,(t) \tag{34}$$

then

$$\frac{d\,\Omega_e}{dt} = (2\,V \cos \eta/r)\,\Omega_e \tag{35}$$

If the change is Ω_e is small enough,

$$\Delta\,\Omega_e = 2\,V \cos\ \eta/r\ (\Omega_e\, T) \tag{36}$$

Solving for the product $\Omega_e\, T$ in Eq. 14 and substituting the result in Eq. 36 yields

$$\Delta\,\Omega_e = 2.8\,\lambda\,V \cos\ \eta/\pi\ r\,\delta_{CR} \tag{37}$$

Hence, to avoid the image smear, we must have

$$\Delta\,\Omega_e = 2.8\,\lambda\ V \cos \eta/\pi\ r\,\delta_{CR} \leq 2\,\Omega_e\,\delta_{CR}/W_{CR} = 2\,V \sin\ \eta\,\delta_{CR}/r\,W_{CR} \tag{38}$$

Hence,

$$\tan \eta_0 = 1.4 \lambda W_{CR} / \pi \delta^2_{CR} \tag{39}$$

2.5.5 Storage Requirements

An important processor parameter is the number of real data values that must be stored. In the image processing situation, an estimate of this value is achieved easily. Each image is formed by taking a one-dimensional Fourier transform of a two-dimensional array of complex data values. One dimension of this array is range; there are as many values in this dimension as there are resolvable points in the unambiguous range window. The other dimension of the array is time, or, equivalently, pulse number. The number of pulses in this dimension is a function of the desired cross-range (or Doppler) resolution. Since there are two real numbers for each complex number, the storage requirements in the processor can be estimated by:

$$S = 2(\text{no. of range cells}) \times (\text{no. of pulses per plane}) \times (\text{no. of planes})$$

$$= 2 N_R (2.8)^2 (W_{CR} / \delta^2_{CR} \pi) \lambda Q^2 P \ln (1/\sin \eta_0) \tag{40}$$

If the number of range cells is made equal to the number of cross-range cells, then

$$S = 2(2.8)^2 (W^2_{CR} / \delta^3_{CR} \pi) \lambda Q^2 P \ln (1/\sin \eta_0) \tag{41}$$

2.5.6 Classification and Identification Processing

So far, it has been assumed that the time required to process each plane is the integration time required to perform the cross-range imaging. It is reasonable to assume that no additional time will be required to perform the imaging in range since pulse compression can be performed in real time before the arrival of the next pulse. The time required for the classification and identification processing, however, must be added to the cross-range imaging integration time, T, to obtain the total processing time. The resulting increase in processing time will lead to an increase in the number of aircraft that must be processed simultaneously, resulting in a corresponding increase in the number of parallel channels required and the number of correlations per second that must be performed. It is not possible to make meaningful estimates of these increases until the algorithms to be used for classification and identification are more completely defined.

2.6 REFERENCES

1. Rafael, M.L., Aircraft Identification by Radar Imaging Feasibility Study, Syracuse University Research Corp., SURC-TR-74-223 (Sept 1974) (Confidential).
2. Herman, R.L., Lothes, R.N., Rankin, P.M., and Wallberg, R.A., Aircraft Identification by Wideband Radar Imaging, Syracuse Research Corp., SRC-TR-77-049 (June 1977) (Secret).
3. Chen, C.C., Imaging with Radar Returns, University of Southern Calif., Image Processing Institute, USC-IPI Report 850 (ARPA Contract No. F-33615-76-C-1203) (Aug 1978).
4. Andrews, H.C., Target Motion Induced Radar Imaging, University of Southern Calif., Image Processing Institute, USC-IPI Report 840 (ARPA Contract No. F-33615-76-C-1203, ARPA order no. 3319) (Sept 1978).
5. Cutrona, L.J., in Skolnik, M.I. (Ed.), "Radar Handbook," Chap. 23, McGraw — Hill Book Co., New York, 1970. (A treatment of the synthetic — aperture algorithm that is closely related to the treatment of the aircraft — imaging algorithm given here.)
6. Davenport, Jr., W.B., and Root, W.L., "An Introduction to the Theory of Random Signals and Noise," Sec. 11-7, McGraw - Hill Book Company, Inc., New York, 1958.

3. SURVEY OF HYBRID OPTICAL/ELECTRONIC PROCESSORS

3.1 INTRODUCTION

Hybrid processing is the technique of combining two dissimilar types of processing systems in such a way that the positive attributes of one system make up for the deficiencies in the other, and vice versa. For the processing tasks at hand, the two types of systems that are to be considered for symbiosis are analog optical processors and digital electronic computers. The attributes of digital computers are well known: they carry out virtually noise-free, highly accurate computations, perform Boolean logic, and offer unlimited flexibility. However, a price must be paid for these services. All sensor data must be converted from some natural parameter (voltage, current, etc.) into a digital data stream. The accuracy of the system is achieved at the cost of vast storage of binary bits. And the flexibility of a computer depends on the cleverness of a programmer or analyst who can model natural systems as equations that are solvable. Finally, each multiplication, each addition, and each data transfer takes time; no matter how fast the machine, the millions of operations required to process data with those clever programs eventually add up.

Analog optical processors have their own positive and negative features. On the negative side, optical processors share with all analog systems a limited quantitative ability and relative inflexibility of design; also, optical processors are nearly useless for performing logical operations. In exchange for these drawbacks, the optical processor offers instantaneous parallel operation on extremely large space-bandwidth product signals. The simple process of shining one image through a second one recorded on a transparency is equivalent to multiplying pair-wise all the points in the two images. Since there are 6×10^6 resolvable image points in a 1-inch square, the power of parallel processing becomes obvious. Other operations for which optical processing is well suited are those that involve the Fourier transform. By a convenient twist of the laws of nature, a Fourier transform relationship exists between the light amplitude distribution in the aperture plane of a lens system and the amplitude distribution in its focal plane. Thus, by inserting appropriate data into the light beam, it is possible to "calculate" instantaneously the two-dimensional Fourier transform of the input data. By application of this property, optical processing systems can be used to perform such diverse tasks as power spectral analysis, matched filtering, correlation, and spectral filtering. The use of cylindrical optical elements permits the decoupling of the two image dimensions. In this way, raster recorded signals may be correlated along one dimension (by matched filtering) while being imaged or Fourier transformed in the other dimension. Of course, for optimization of these operations, clever system design and setup in the optical processor is as important as clever programming is in the digital computer. Table 3-1 shows which operations are best performed digitally and which should be suitable for optical processing.

Table 3-1 — Appropriate Processing Tasks

Optical	Digital
• Multiplication	• Noise removal (subtraction)
• Correlation	• Thresholding (comparisons)
• Fourier transforms	• Mensuration

	• Control functions
	  • Formatting
	  • Selection of operations

Optical processing has not yet made a significant impact in most fields because of two related problems. First, the output of most optical processors is nearly useless without further interpretation. An arrangement of light spots is simply not meaningful; this is the impetus for hybrid processors. Second, until recently, it has been very difficult to enter data into and extract data from coherent optical processors. This lack of interface devices to connect the optical system to the rest of the electronic processing world has impeded the development of hybrid systems, but advances in spatial light modulator and charge-coupled device technology have opened many avenues for computer-optical system interaction.

In this section some representative hybrid processing systems will be discussed in order to present the current level of performance available.

3.2 POWER SPECTRUM AND DIFFRACTION PATTERN ANALYSIS

Some of the first hybrid optical/electronic processing systems were developed to perform either power spectrum or difraction pattern analysis. In power spectrum analysis, a collimated beam of monochromatic light is passed through the input information, which is usually in the form of a photographic transparency (e.g., an aerial photograph). A lens is used to collect the light and to form an intensity distribution that is a representation of the spatial power spectrum of the input data. This property is the so-called Fourier transforming property of lenses and is easily derived from diffraction theory. The spatial location and relative strengths of the bright areas in the intensity distribution are measured with some detection system and sent to the computer for further analysis. This analysis is usually based on the spatial spectrum of known classes of targets.

Diffraction pattern analysis is essentially the same process as power spectrum analysis, but the input data for diffraction pattern analysis are three-dimensional objects. The light passing by the objects is diffracted by the edges and surface textures of the objects and the lens form a real image of the far field diffraction pattern. The detected information about the diffraction pattern is again analyzed by an electronic computer.

These types of analyses exemplify the philosophy inherent in hybrid processing. The first part of the process—the calculation of the power spectrum or diffraction pattern—is an inherently time consuming operation for an electronic system because of the required parallel to serial conversion of data. Optically, this "calculation" takes place literally at the speed of light once the data is in place. On the other hand, the analysis of the spectrum or diffraction pattern is almost impossible to perform optically. This constraint is true no matter how simple the analysis. Even threshold detection or the comparison of the values at two frequency points — operations that do not require digital computations—are beyond an optical system's capability. For an electronic system, these operations are trivial. If a digital computer is involved, analysis algorithms of much greater complexity can be utilized.

Some of the diffraction pattern or spectrum analysis systems that have been built will be discussed below.

3.2.1 Cytological Cell Screening

Recently, Pernick, et al.,[1]* have discussed a hybrid processing system that incorporates many of the features of other power spectrum analyzers. This processor, designed to perform cytological cell screening on Pap smear samples, is shown in a schematic representation, Fig. 3-1a. A magnified cell image (100×) is formed on the active surface of an incoherent-to-coherent converter by a projection microscope. An expanded laser beam is spatially modulated by the image stored on the transducer and a suitably scaled power spectrum is formed by the transform lens on the surface of the ring and wedge detector.

This ring and wedge detector, manufactured by Recognition Systems, Inc., has become a standard element in these types of hybrid processors. The detector is circular, consisting of 32 angularly spaced wedge-shaped elements covering 180 degrees and 32 semicircular, radially spaced elements in the remaining 180 degrees. Because all power spectra of interest have 180-degree rotational symmetry, the rings and wedges sample equivalent data. For Pap-smear processing, the designers of this system determined that the greatest cell parameter discrimination is obtained when the angular variations are measured in the restricted window of 509 to 600 cycles per millimeter. Thus the wedge elements were masked to accept light in that passband only, as shown in Fig. 3-1b.

The data from each of the 64 detector elements is sampled at appropriate times and stored on magnetic tape for subsequent digital processing. In operation, at least three sets of measurements are made for each cell: zero light (i.e., dark current) measurements, clear aperture (energy normalization) measurements, and cell power spectrum measurements. After these data are collected, the optical portion of the processing is complete and the electronic digital processor takes over. It should be noted, however, that the timing and sequencing of the elements in the optical system are also under electronic control.

The electronic processing of the power spectral data is divided into two areas. The first area is data rectification; the data from the elements is weighted by a predetermined sensitivity factor, the dark current bias is removed, and the energy calibration data is used to normalize each signal.

The second area of electronic processing is statistical. It was demonstrated that six easily derived cell transform features perform quite well as discriminators using standard Bayesian decision algorithms with quadratic decision rules. The six-cell transform features used in this system are, of course, quite specific to the cell screening problem and cannot be applied to the general power spectrum analysis problem. For completeness, these features are listed in Table 3-2.

The results achieved with this system are quite encouraging. The degree of separation of abnormal from normal cells is essentially identical to an equivalent film-based system in which a 2 percent false negative rate with a corresponding 17 percent false positive rate has been achieved. (Hand screening methods are reported to be comparable with a 3 percent to 25 percent range.)

---

* References are listed in Section 3.5

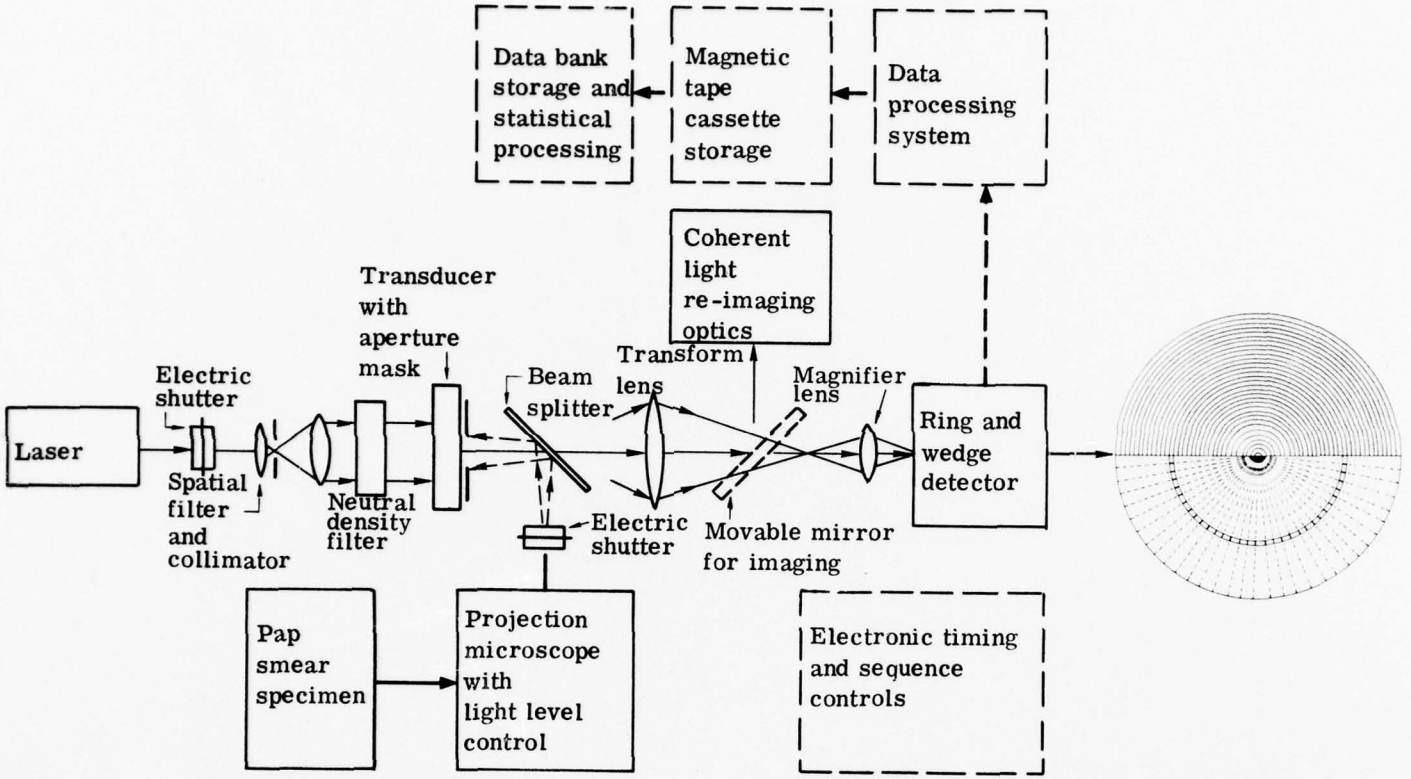

(a) Schematic diagram

(b) Detail drawing of ring and wedge detector (masked)

Fig. 3-1 — Cytological cell sorting hybrid processor

Table 3-2 — Discriminant Features Used for Malignant/Normal Cell Classification

1. Total energy in the sample Fourier transform spectrum
2. Slope of the quantity $\rho^2 |F(\rho)|^2$ in the 10 to 40-cycle/millimeter range, averaged over the polar angle θ and normalized to the total energy
3. Variance of the radial distribution $|F(\rho)|^2$ in the 10 to 100-cycle/millimeter range, averaged over the polar angle θ and normalized to the total energy
4. Variance of the quantity $\rho^2 |F(\rho)|^2$ in the 10 to 100-cycle/millimeter range, averaged over the polar angle θ and normalized to the total energy
5. Variance of the angular distribution $|F(\theta)|^2$, averaged over the 500 to 600-cycle/millimeter range
6. Harmonic content in a portion of the power spectrum of the angular distribution $|F(\theta)|^2$, averaged over the 500 to 600-cycle/millimeter range

Note: $|F(\rho,\theta)|^2$ is the power spectrum in polar coordinates.

3.2.2 Cloud Screening

A second area to which hybrid power spectrum analysis is being applied is the screening of aerial photographs to determine the degree of cloud cover. The need in the mapping community for fast, automated cloud screening procedures comes from the challenge of effectively utilizing increasingly large volumes of aerial photographs to provide maps to decision makers in a timely manner. The major effort in this area has been undertaken by the U.S. Army Engineer Topographic Laboratories. The first stage of this effort, as reported by Lukes,[2] was the development of a breadboard recording optical spectrum analyzer (ROSA) so that samples of the filmed imagery could be processed to produce a power spectrum data base. This data was then used to test the efficiency of different feature extraction and classification algorithms. In addition to testing the classification software, this ROSA had a variable sampling aperture to permit the evaluation of the effect of image sample size on cloud cover discrimination.

The hardware incorporated in the ROSA consisted of fairly standard coherent optical system components and the ubiquitous ring-and-wedge detector. Output data was recorded on punch cards for statistical processing in a CDC 6600 computer. Standard procedures such as energy normalization were applied.

The results of these experiments demonstrated several points:

1. Classification results are strongly dependent on sample aperture size. Smaller apertures result in more homogeneous samples and more unambiguous optical power spectra.

2. Definition of classes (based on training data set) exerts a strong influence on classification results. Homogeneous training patterns provide the most dependable performance.

3. For the sampling parameters used, a two-class discrimination (cloud/no-cloud) can be achieved with 95 percent accuracy using a three-component feature vector using any of four different classification algorithms.

4. The majority of misclassifications in this data base were the mislabeling of grasslands as clouds. At the scales involved, grasslands appear homogeneous and are thus very similar to clouds. It was suggested that the reflectance data lost in normalization might reduce these misclassifications.

The second stage of this cloud screening program is to incorporate the results of the breadboard experiments in automated systems that scan film, classify the image, and file the data. In this way, clear (i.e., cloudless) imagery of specific regions can be found in a "library" of film on short notice. To further the development of this system, the Topographic Laboratories has been working on a large telecentric laser scanning system designed for use with the high speed optical power spectrum analyzer.[3]

3.2.3 Particle Size Analysis

Just as two-dimensional objects can be classified by analyses of their power spectra, so too the Fraunhofer diffraction patterns caused by light passing by three-dimensional objects can be analyzed to determine the nature of the objects. One class of objects to which this technique has been successfully applied is fine particulate matter. Leeds and Northrup Corporation has created a hybrid optical/electronic processor using this principle to create a commercially available industrial instrument.[4] The basic concepts of this instrument are discussed below.

Fig. 3-2 shows a schematic of the optical system used in this processor. As with the power spectrum analyzers discussed above, a collimated beam of laser light is passed through a cell containing the particles being tested. Unlike the cell sorting and cloud screening applications, in which the class of each cell or each image patch was to be labeled, particle size analysis is a task in which the statistical properties of a batch of particles are under test. Thus the sample cell holds many particles, with the only limitation being that the particle density be low enough to avoid multiple scattering. The scattered light is collected by a lens and focused into the plane of a rotating, three-segment mask. The light passing through the mask is then detected on a single detector.

The purpose of the rotating mask is to generate a sequence of three signals, S_1, S_2, and S_3, proportional to the second, third, and fourth moments of the number density distribution by radius (that is, the function that describes the percentage of particles having a particular radius). The holes in the mask needed to produce these signals are (approximately) wedge shaped, radial slit shaped, and arc shaped. In addition to generating the moments of the number distribution, the three signals can be combined to produce other statistical measures of the sample of particles. The distribution parameters that may be measured are shown in Table 3-3.

Table 3-3 — Measurable Particle Distribution Parameters

Total cross-section area
Total surface area
Area mean radius
Area standard deviation
Total volume
Total mass
Volume mean radius

These various statistical measures are calculated by a microcomputer that accepts the digitized versions of the three signals. The output is in the form of both visual display using light-emitting diodes, and hard copy via a printer. The system maintains its linearity for particles with a range of sizes from 2 to 100 micrometers, and is capable of making rapid, continuous measurements on a flowing particle distribution.

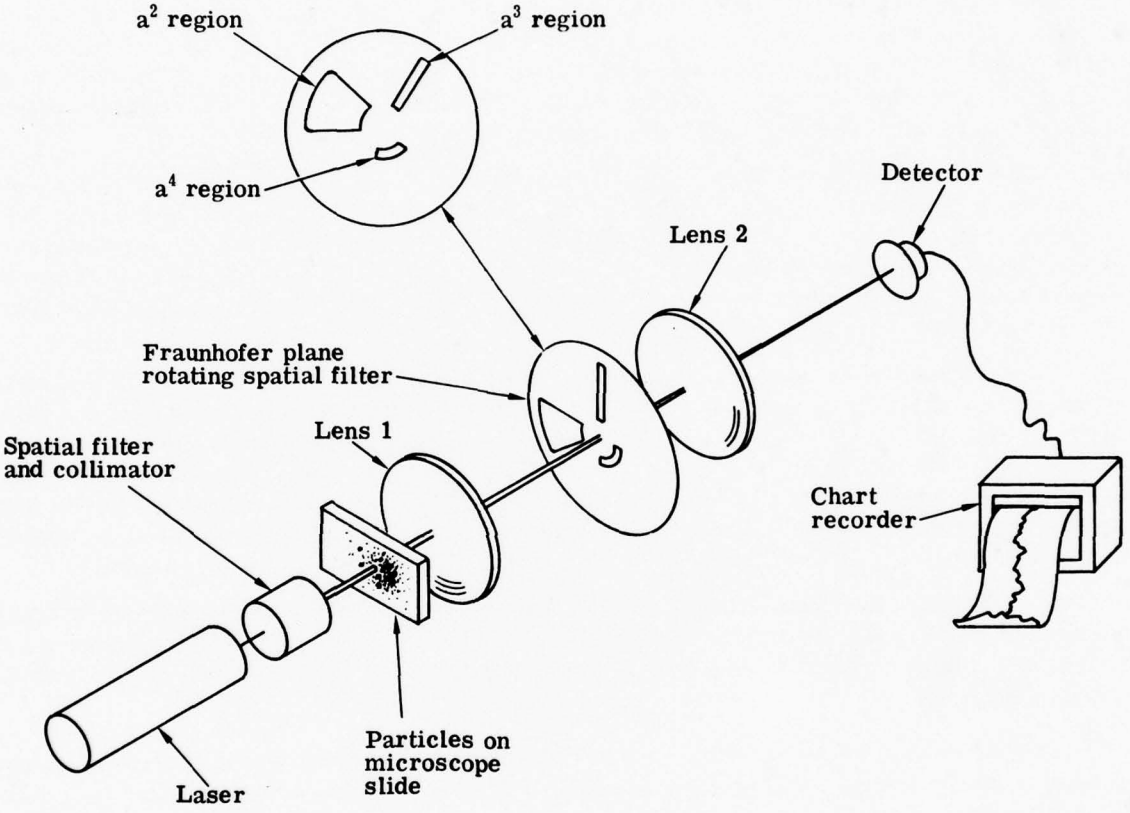

Fig. 3-2 — Hybrid particle size analyzer

3.2.4 Spectral Analysis of One-Dimensional Signals

An important class of hybrid spectrum analyzers are those designed to process radar or other one-dimensional time-varying signals. In theory, these processors are just degenerate forms of those discussed above because the dimensionality of the input signals is reduced from two to one. In practice, the engineering problems and processing requirements of a radar signal spectral analyzer are so different from a particle size analyzer or cloud cover screening system that a one-dimensional system becomes a unique processor in its own right.

Unlike the classification systems for clouds, cells, or particles, which measure the coarse distribution of energy in the spectral plane, a radar spectrum analyzer is usually required to precisely measure the energy in each resolvable frequency bin. Similarly, the window in a classification system usually just defines the field of view of the system, but the window in a radar processor affects the resolution the frequency measurements of systems by changing its time-bandwidth product.* Finally, the input signal to a classification system usually is already in an optical format (e.g., aerial photograph) whereas the input to a radar signal processor must be converted from a time-varying electrical signal to a spatially varying optical signal.

The impact of these differences is felt most heavily at the two ends of the spectrum analyzer: the input and output transducers. The low resolution ring and wedge detector (which is so useful in classification systems because it spatially integrates frequency data radially or angularly) is of no use. Instead, high resolution rectilinear arrays of detectors must be utilized to measure the precise energy distribution in frequency space. Conveniently, such detector arrays exist because of the rapidly advancing CCD technology.

At the other end of the spectrum analyzer, the input transducer that converts the electrical signal to an optical signal is the key element that defines the operating parameters of the entire system. The most popular input transducer for this application is the acousto-optic (A-O) Bragg cell. In the A-O cell, variations in the electrical signal are used to launch sound waves through a crystal. The phase delays caused by the index of refraction changes associated with the sound waves represent a nonlinear optical representation of the electrical input. Under many conditions, however, the representation is close to linear and thus is useful for spectrum analysis.[5]

A major limitation of A-O cells is their small time-bandwidth product. Because of acoustic attenuation and dispersion, attempts to increase the bandwidth of the signal are nullified by a shortened useful time window. Fig. 3-3 shows the operating ranges of A-O cells made from different materials.[6]

In spite of this difficulty, many companies offer radar spectrum analysis systems based on acousto-optic diffraction. The primary advantages of these systems are their speed (as compared to digital systems) and simplicity. Known as instantaneous Fourier transform processors, the commercially available systems have impressive specifications. Itek's series 200-1 IFT processor simultaneously collects all CW and pulse signals in a 500-MHz bandwidth with an optical

---

* The time-bandwidth product is a measure of the information handling capacity of a signal processing system. For example, consider a spectrum analyzer that has a time window T seconds long and that can accept signals with temporal frequencies from dc up to B cycles per second. From Fourier theory, the resolution of the analyzer, R, is proportional to 1/T, so the number of resolvable frequency bins, N, is the maximum frequency that the processor can handle divided by the resolution cell width:

$$N = \frac{B}{R} = TB \equiv \text{time-bandwidth product}$$

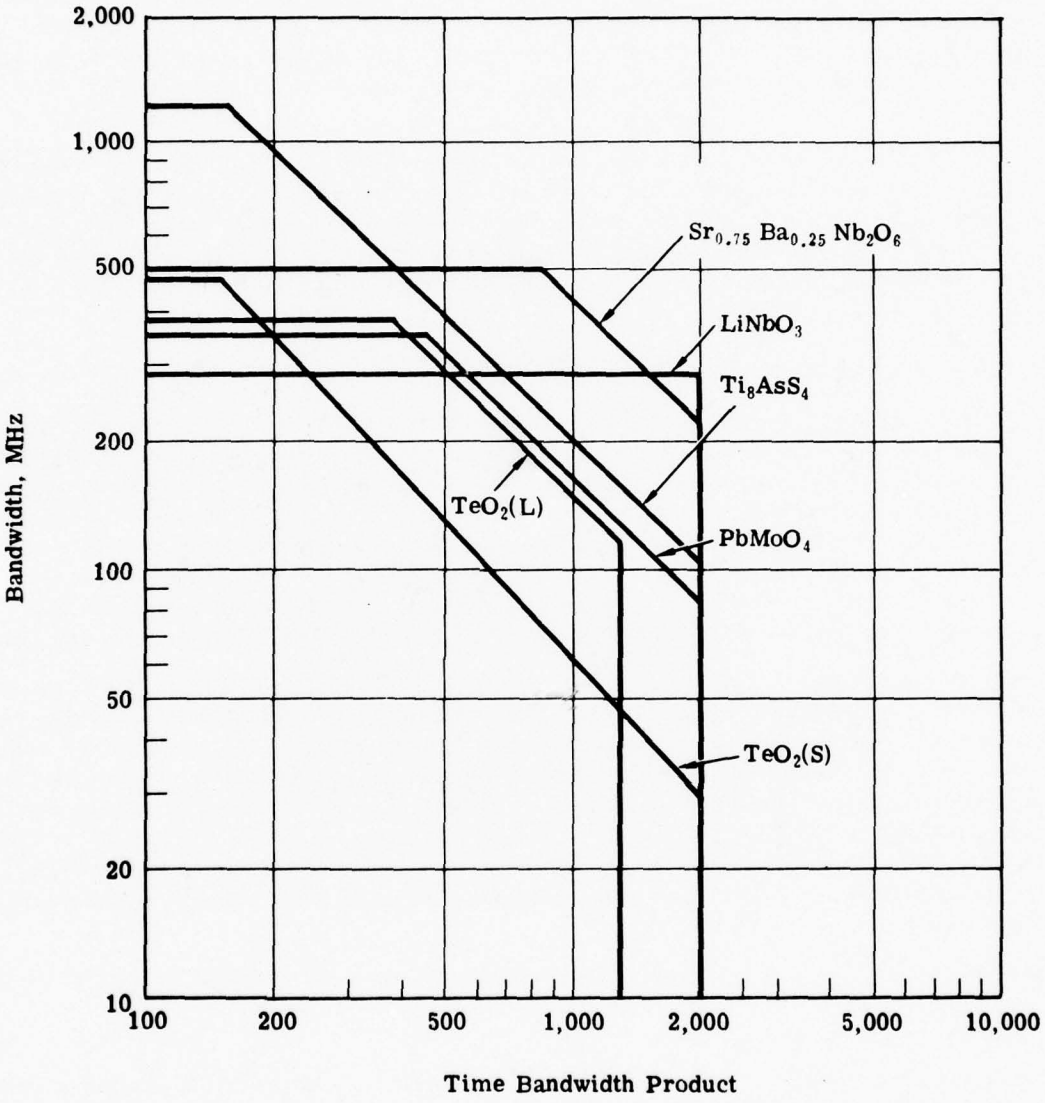

Fig. 3-3 — Acousto-optic Bragg cell characteristics

resolution of 1 MHz. It is capable of characterizing agile emitters for chirp, glide, hop, or random modes. A GTE Sylvania processor measures 11 × 19 × 4 inches and has a 1-GHz bandwidth with 2.5-MHz frequency resolution. ESL has built a system with a 2.8-GHz center frequency, 884-MHz 3-dB bandwidth, and a 500-KHz resolution.

While the basic limitation on the A-O spectrum analyzer is low time-bandwidth product, this limitation does not apply to all hybrid spectrum analysis systems. If the one-dimensional electrical signal can be reformatted as a two-dimensional raster, then the time-bandwidth product of the optical spectrum analyzer can be increased by a factor equal to the number of lines in the raster. It is relatively easy to show that the raster formatted signal results in a raster formatted spectrum.[7]

The difficulty encountered with this concept is the need for a two-dimensional input transducer. Efforts have been expended on stacked A-O cells, high speed scanners (onto reusable transducers), and the like, but no truly satisfactory (i.e., simple and inexpensive) solution has been developed. However, in the special circumstances where line by line recording of the incoming signal onto expendable material is permitted, the raster recording technique allows very high resolution spectra to be obtained.

3.3 FOURIER TRANSFORM PROCESSORS

While power spectrum and diffraction pattern analyzers are the most prevalent hybrid processors in use today, the power of hybrid techniques is probably best demonstrated in Fourier transform processors. In these systems the Fourier transforming property of a lens is used to access the spectrum of the input image. The spectrum is then modified by a filter, and the modified spectrum is retransformed to create an enhanced image. This type of processing may be contrasted with the spectrum analyzers in which the data of interest was just the spectrum itself. Since the Fourier transformation process is instantaneous in an optical system, the throughput rate of a hybrid processor is limited only by the input/output transducers and the filter selection process.

A prototypical Fourier transform processor is shown in Fig. 3-4. A coherent beam of light passes through the data in the input plane and the spectrum of the data appears in a plane between the two lenses. A spatial filter in this plane modifies the spectrum in a predetermined manner. This filter could be as simple as a binary bandpass filter or as complicated as a matched filter (i.e., one with a complex amplitude transmittance proportional to the conjugate of the spectrum of a target of interest). The light leaving the filter is retransformed by the second lens to create a modified image in the output plane. The "modified image" might retain an image-like appearance or it might be a bright spot that represents the cross-correlation between the input image and a reference image.

In the sections that follow, several hybrid Fourier transform processors are discussed.

3.3.1 Moving Target Indicator

Von der Ohe, et al.,[8] have described a coherent optical processor which is used to detect and locate objects in the sky that move relative to the background of fixed stars. A time exposure of the sky, with the imaging system stabilized on the stars, will result in two types of images: points representing the fixed stars, and streaks representing moving objects. Space-invariant pattern recognition may be performed on such a composite image if the Fourier transform of the image is passed through a filter that is "matched" to the streaks. This filter is simply a slit that can be oriented along the direction perpendicular to the direction of the streaks.

This filter discriminates against the fixed star background in favor of the target streaks in two ways. First, the slit transmits only a small fraction of the energy from the rotationally uniform spectra of the fixed stars and noise, whereas it transmits a large fraction of the energy from

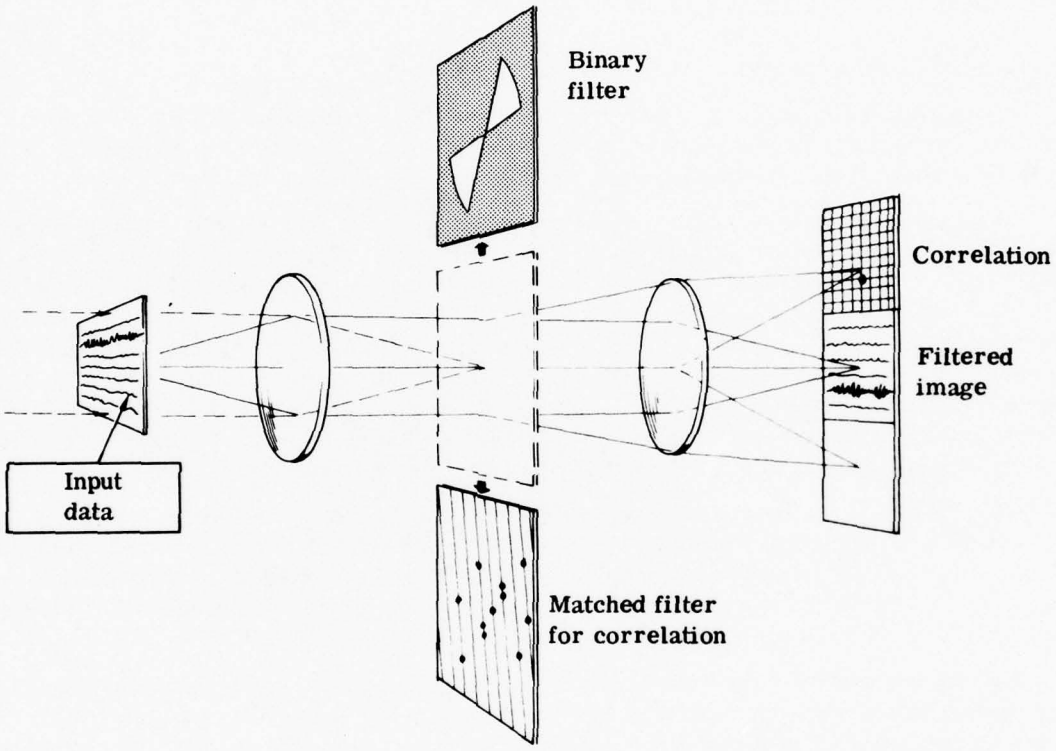

Fig. 3-4 — Prototype Fourier transform processor

the targets (when the filter is aligned). Second, if the filter is rotated continuously, then the energy transmitted due to the targets oscillates widely at the angular frequency of the filter but the energy due to the fixed stars is more or less uniform. Thus, the presence of a target is indicated by the ac component of the transmitted energy and the direction of the target movement is indicated by the phase of the ac signal relative to the filter drive signal.

The coarse position of the moving target is recovered in this system through the use of an array of detectors in the output image plane. The amplitude and phase of the ac signal from each detector is processed individually to localize a moving target in the sector of the sky corresponding to that detector. The resolution of the array is limited by the expected streak length.

An experimental demonstration of this system has been performed using film as the input plane medium. To become a useful system, a real-time capability is required, so a breadboard system using an Itek PROM is being designed.

3.3.2 Ground Target Recognition

A second class of Fourier transform processor was demonstrated by Grumet, et al.,[9] of Grumman Aerospace. They developed an optical matched filter correlator designed for ground target recognition that they tested against model and field generated imagery.

The Grumman system is shown in the schematic diagram in Fig. 3-5. While most of the components in the schematic may be identified in terms of the prototype processor in Fig. 3-4, several unique features of this system must be explained. The most outstanding feature is the "hololens," a 3 × 3 array of holographically prepared lenses that breaks the beam from the input plane transducer into nine replicated Fourier transforms. Each of these transforms is filtered individually by one of the filters in the matched filter memory bank. The memory bank is prepared by masking all but one transform position and presenting the film in the filter plane with a uniform reference beam and the reference target transform simultaneously. The nine memory locations are all exposed with different references before development.

This system is configured to accept incoherent images from either transparencies or from a projection TV. (The projection TV is driven from a night vision device.) For the experiment of interest, all imagery was generated through the night vision device and a TV monitor, photographed on 35-millimeter film, and projected onto the transducer with a xenon arc. The quality of the projection TV was inadequate for this type of processing.

Several types of imagery were prepared for the demonstration experiment. Model images of a tank and of a truck were made on a test stand, and field images of a tank and a truck were made with and without electronic enhancement. (The electronic enhancement basically consisted of hard clipping.) Matched filters were prepared for different ranges and aspect angles using both model and field imagery. These filters were then used to process similar imagery. Table 3-4 shows the results of these experiments. "Tracking" in the table was determined by using input images that had the target in various locations across the field of view.

The ability to obtain correlation and tracking with an optical system has been demonstrated by this experiment. Simultaneously, systems analyses were performed to evaluate the effects of using both high and low pass filters (only high pass were used in the experiment), of recording multiple filters at each memory location, of the effect on target range resolution on memory size, etc. Such studies resulted in projections that a 2 × 2-inch filter plane could store 8,000 filters, and that these 8,000 filters would be adequate for a perimeter penetration warning system for four targets which might be expected in a 1 to 2-kilometer range.

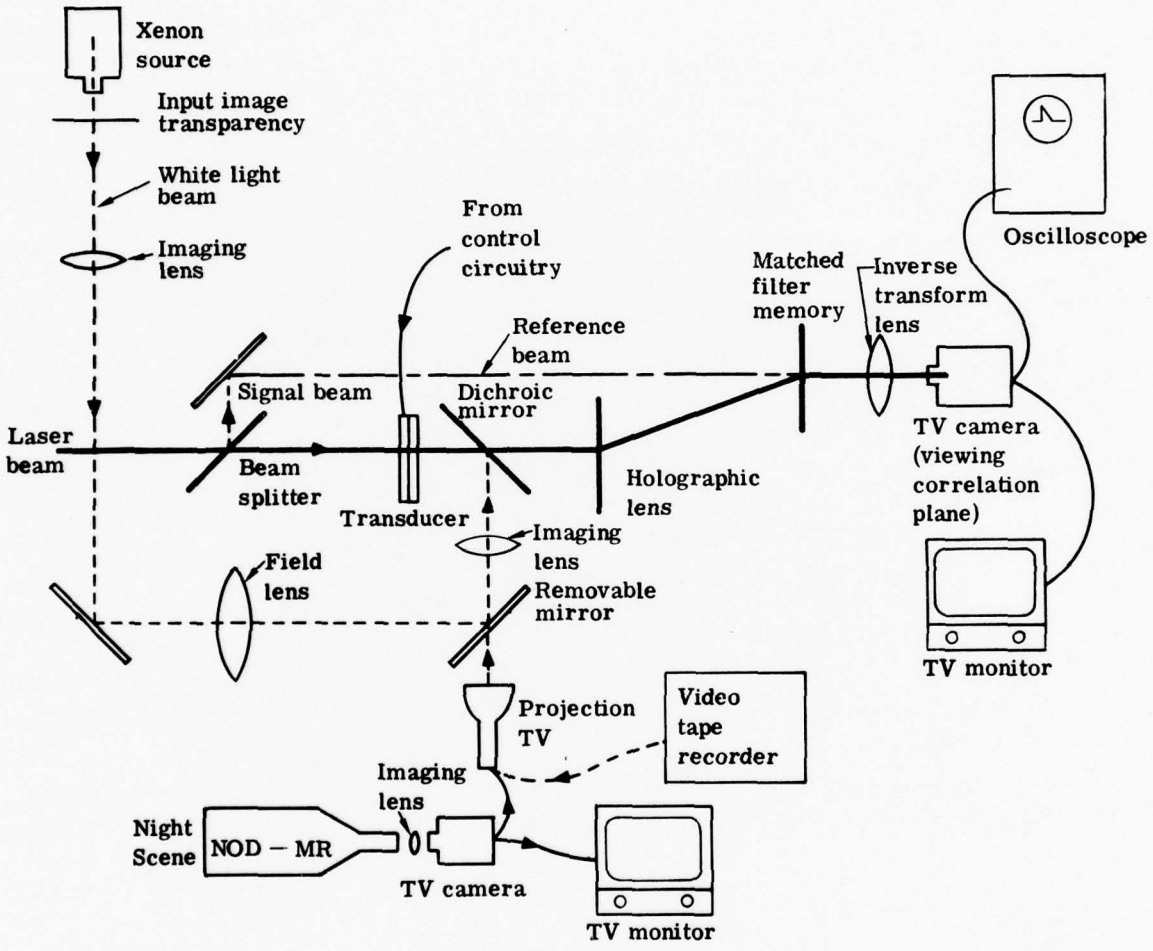

Fig. 3-5 — *Ground target recognition system*

Table 3-4 — Xenon Imagery Playback Optical Matched Filtering

Matched Filter	Input Image	Correlation Signal, volts	Noise Peak, volts	Average Noise, volts	Signal/ Peak Noise	Signal/ Average Noise	Tracking
Truck model	Model	0.7	0.07	0.01	10	70	Yes
0.62 km, 90°	Enhanced video	0.6	0.16	0.01	4	60	Yes
	Unenhanced video	0.8	0.2	0.04	4	20	Yes
Truck model	Model	0.75	0.2	0.04	4	20	60%
0.62 km, 0°	Video	0.85	0.5	0.15	1.7	6	50%
Tank model	Model	0.5	0.02	0.01	25	50	Yes
0.9 km, 90°	Enhanced video	0.13	0.025	0.01	5	20	Yes
	Unenhanced video	0.75	0.15	0.02	5	37	Yes
Tank video	Enhanced video	0.5	0.02	0.01	25	50	Yes
0.62 km, 90°	Model	0.18		0.04		5	60%
Tank video	Enhanced video	0.85	0.3	0.04	3	21	Yes
0.62 km, 0°	Model	0.5	0.2	0.04	2.5	12	Yes
Tank video	Enhanced video	0.7	0.04	0.01	18	70	Yes
1.4 km, 90°	Unenhanced video	0.8	0.15	0.04	5	20	Yes

3.3.3 Two-PROM Processing System

One of the difficulties with Fourier transform processing systems has been their relative lack of flexibility since a different spatial filter is required for each operation. A second difficulty associated with coherent spatial filtering systems is the requirement that the input image be in the form of a spatially varying amplitude transmittance; both the magnitude and phase of the input must be controlled. In practical terms this restriction has meant that printed images, TV images, and the like could not be used at all, and that images stored as transparencies should be used only if liquid gated.

These drawbacks can be overcome if the Itek PROM is used in both the input and spatial filter planes of the processor. As a demonstration of this PROM application, Itek assembled the two-PROM optical processing system shown in Fig. 3-6.[10] The input transparencies were imaged onto the input plane PROM with a mercury arc lamp, and the Fourier plane PROM was addressed with a spot of 476-nanometer light from a krypton laser. The beam was modulated with an A-O modulator and X-Y deflected with an A-O deflector and a galvanometer. Minicomputer-controlled electronics were used to create circular low pass, high pass, ring, wedge, and shaded spiral spatial filter patterns. Examples of low pass filtering are shown in Fig. 3-7. A bar target image is shown with the cutoff of the low pass filter first set to pass the zero order only in (a). The bandpass of the filter was then increased sequentially in (b) through (e).

It should be noted that with a single Fourier plane PROM it is not possible to obtain independent control of the magnitude and phase of the filter transmittance. There exists one special case of phase modulation that may be obtained: by the use of baseline subtraction, parts of a filter may be made to have negative amplitude transmittances, i.e., π phase. If, for example, the differentiation filter $T(k_x) = i\,k_x$ were desired, then the biased intensity ramp $k_x + k_0$ would be scanned onto the PROM. The bias in the image would then be removed with baseline subtraction, resulting in a positive ramp in one half-space and a negative ramp in the other.

3.4 RADAR SIGNAL PROCESSORS

The final class of hybrid optical/electronic processors that will be discussed are those designed to process radar signals. These include processors used to generate imagery from synthetic aperture radars and those designed for range/Doppler processing of pulsed radars.

3.4.1 Synthetic Aperture Radar Processors

One of the more spectacular successes of optical processing techniques has been the generation of imagery from synthetic aperture radar (SAR) returns. There is not adequate space to describe all the processing requirements of SAR or to prove that optical processors can perform all the required operations. Suffice it to say that an electromagnetic analogy exists between the complex amplitude of the radar signal received at the airplane over a period of time and the light amplitude that would be recorded in space if a hologram were being made of the same scene. In effect, it is possible to record the radar returns to make a hologram of the ground using microwaves instead of light. This hologram may be read out using coherent light to form a real image of the ground. In practice, the hologram is anamorphically distorted by the ratio of the speeds of light and of the plane to the X and Y scanning speeds of the recorder that converts received radar signals to amplitude transmittance variations on the hologram material (i.e., film strip).

In general, when the hologram is illuminated with coherent light the real image for the range dimension is focused into a different plane from the image for the cross-range dimension. Additionally, the focal plane is generally a function of the range, and the magnification in the two directions is anamorphic. The optical processors for SAR systems must reimage the real holographic image while removing all of these distortions. These processors are made up of various spherical and nonspherical lenses, with the specific combinations determined by various factors such as the radar waveform used to form the hologram originally.

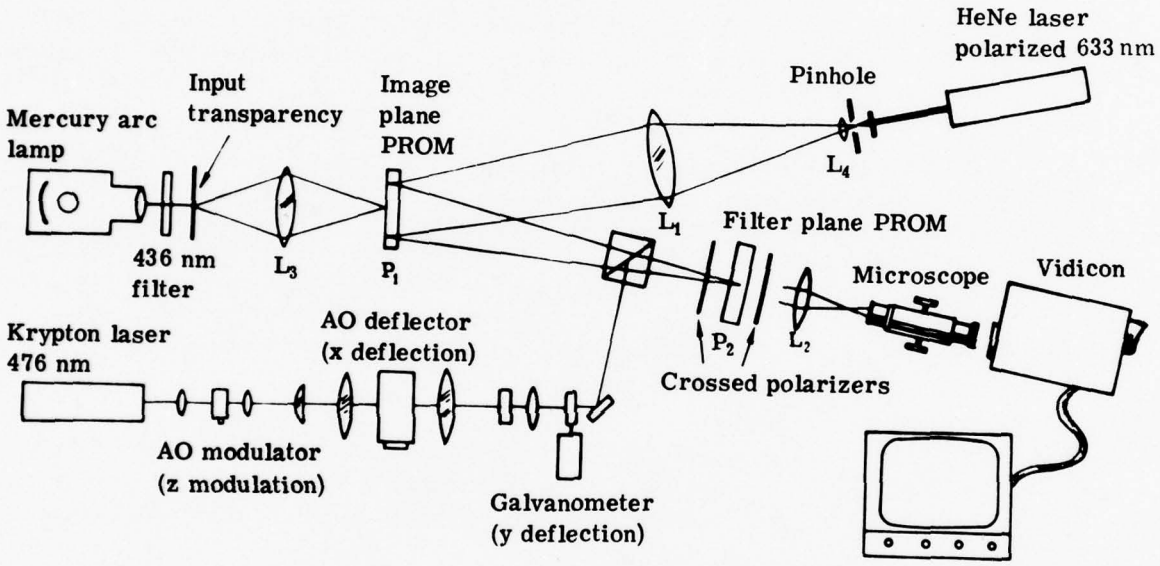

Fig. 3-6 — Two-PROM processing system

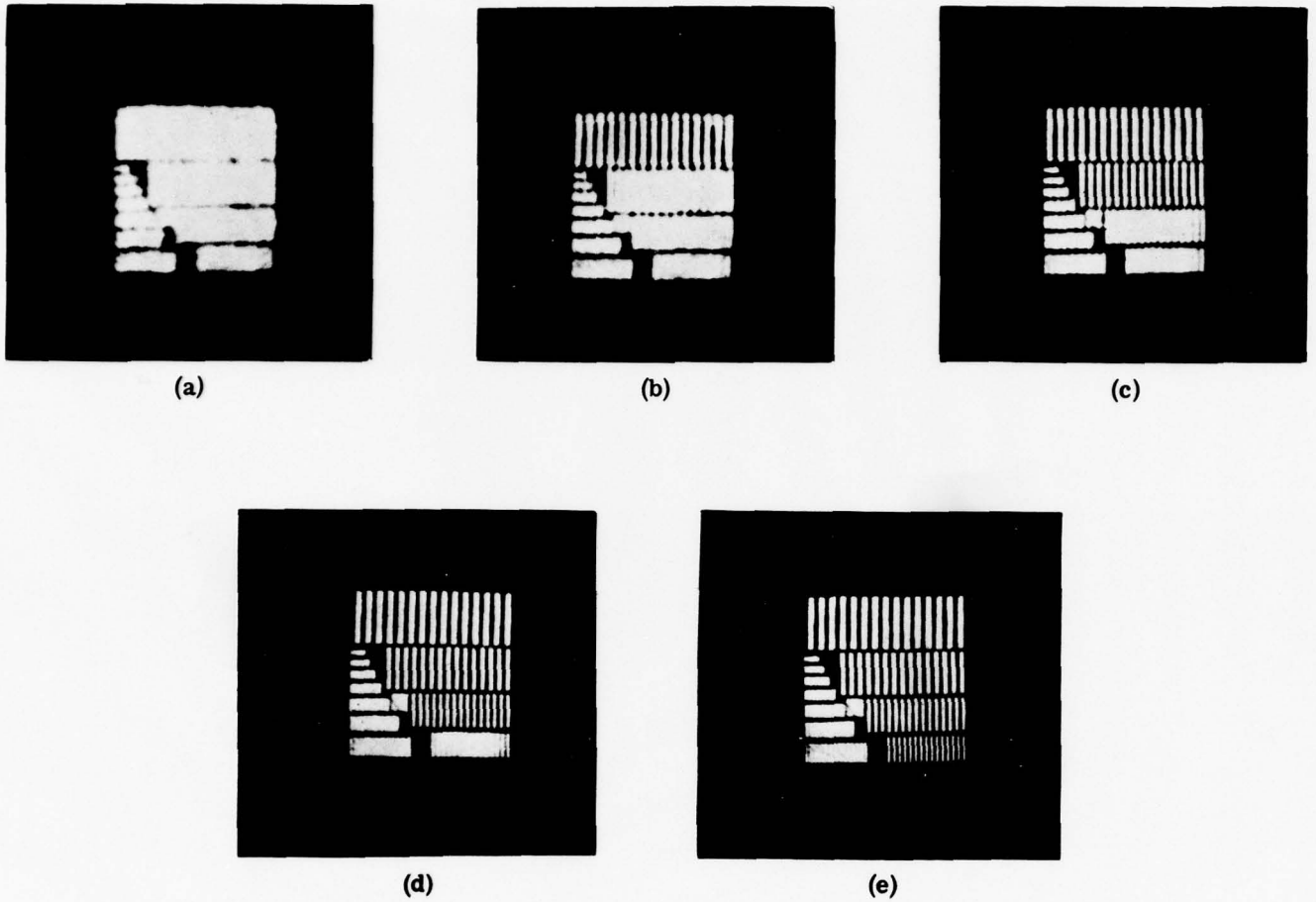

Fig. 3-7 — Real-time low pass filtering of a resolution target: cutoff frequency increasing from a to e (after Iwasa)

While the specific designs of SAR processors will not be discussed, these processors are important because they bring to light two important factors about hybrid processing systems. First, these processors are currently being used in everyday work situations by the Defense Mapping Agency, Jet Propulsion Labs, and others. In terms of the cost-performance tradeoff, JPL has selected a new hybrid processor for the SEASAT program because it was cost-effective. It is reported that the hybrid system will generate images in 10 minutes that a 2 to 3-million-dollar digital system would require 16 hours to produce. This success is due to the proper matching between processing requirements and system capabilities. The second factor is that all of the SAR processors are film based, which is to say they operate in "delayed" real time. It is generally true that fully hybrid processors — those in which the digital and the optical processor interact fully — have not been developed because of a lack of suitable electrical-to-optical data converters. The transducers that are available can be used to demonstrate processing techniques, but they cannot be utilized in the extremely high time-bandwidth product, high data rate processing tasks that makes hybrid processing effective.

Fig. 3-8 is a comparison of existing optical and digital processors for SAR using a figure of merit called the "equivalent complex multiplies per second per dollar."[11] An important point to remember in viewing this chart is that all the optical systems are special purpose machines made to match the processing loads of particular radar systems. These systems could all have increased figures of merit if the film transport systems were improved and the lasers (which are now about 10 milliwatts) were made brighter. The 2×10^7 line on the chart indicates the estimated limit with 1977 technology.

3.4.2 Range-Doppler Processor

The second type of radar processing that will be discussed is so-called range-Doppler processing. In reality, this processing is a generalized form of SAR processing and is almost identical to HR^3 image generation. The particular range-Doppler problem that has been addressed by an optical solution is the tracking of re-entering ballistic vehicles. As is typical, high range resolution is achieved using pulse compression techniques, and velocity measurements are achieved by observing the Doppler shift on each returning pulse. Because the pulse is short, the Doppler shift in frequency appears to be just a phase shift on the returning carrier. To measure this apparent phase shift, a minimum of two sequential returns from any target must be compared, but higher Doppler (i.e., velocity) resolution is obtained when many returns are compared.

A hybrid processing system to perform real-time range-Doppler processing has been built by Ampex for BMDATC.[12] Fig. 3-9 is a diagram of the processor. The input radar signal, after being converted to an appropriate IF carrier, is fed into a Bragg cell which is illuminated by a laser. The Bragg cell is imaged onto a liquid crystal light valve on which is stored an adaptable reference signal. A stop in the optical system converts the phase signal into an intensity varying image.

As the signal propagates through the Bragg cell, the image slides across the reference, producing the sliding product. A lens integrates the product, and the resulting correlation signal is received by a photo-detector. This signal is a series of pulses, one for each target.

These compressed pulses are then Doppler processed. Each string of return pulses (from one outgoing pulse) is written on a single line of a second light valve. After 300 lines have been written, a one-dimensional Fourier transform is performed perpendicular to the lines and the line-to-line Doppler phase shift causes the focused spot in the Fourier plane to move upward by an amount proportional to the phase shift. In the along-line dimension, the compressed pulses are imaged, so the output display is a mapping of the range and velocity of the targets.

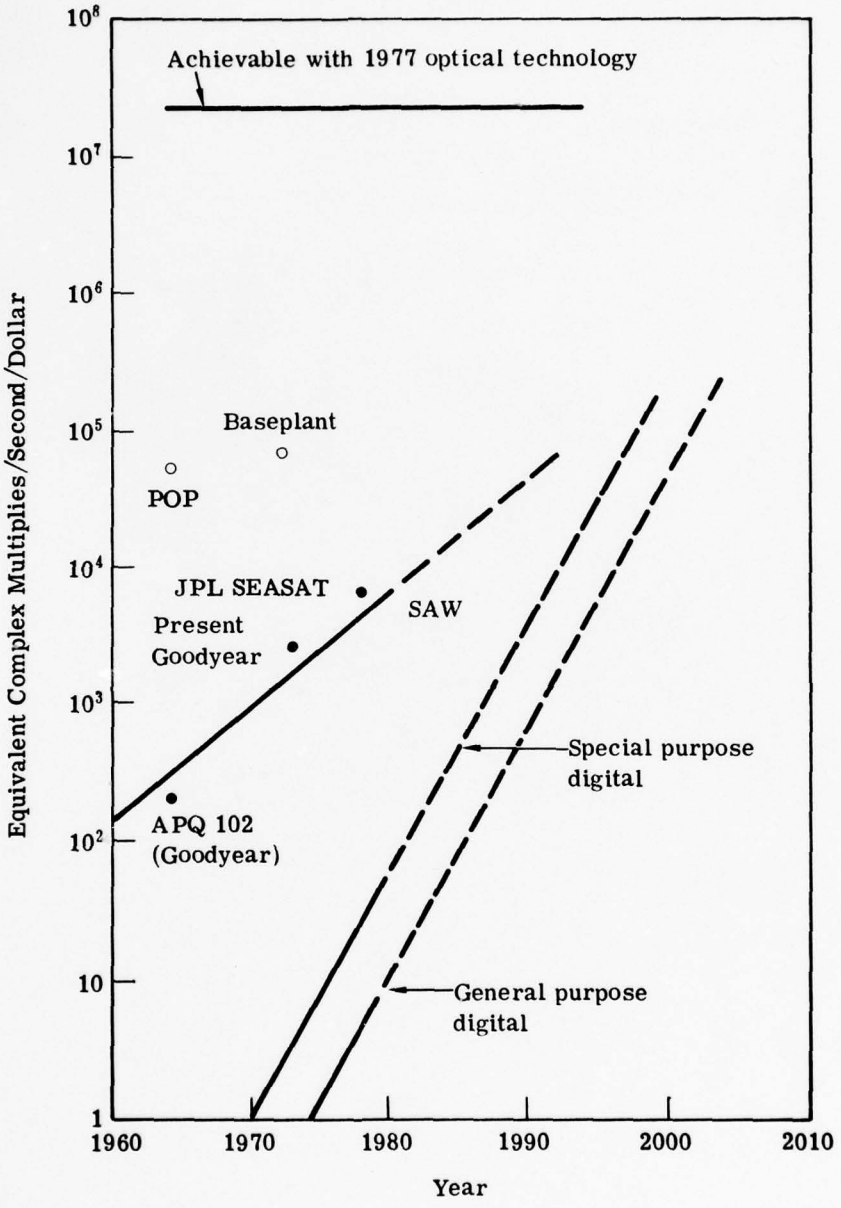

Fig. 3-8 — Trend lines for various SAR processors

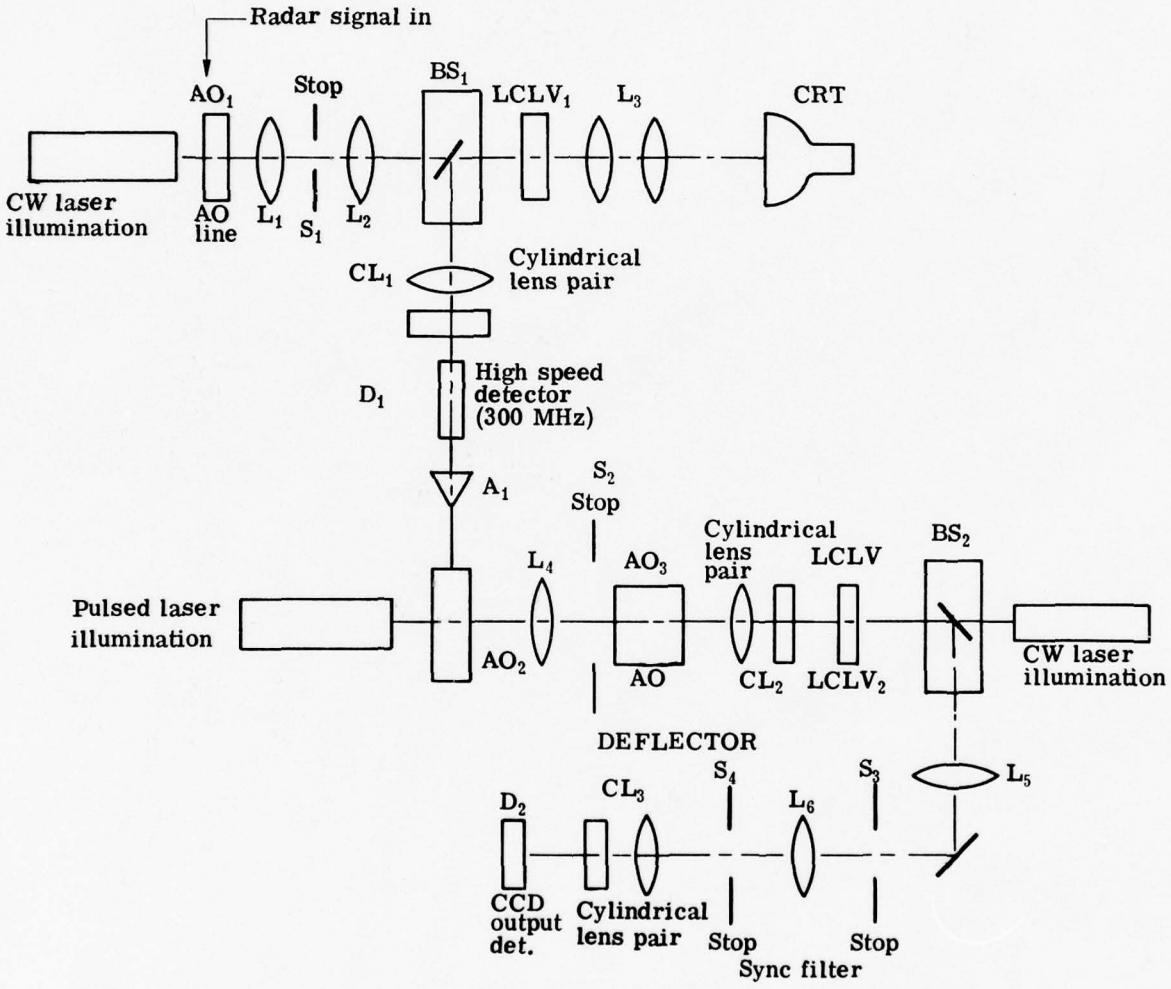

Fig. 3-9 — Schematic of Ampex-BMDATC hybrid radar processor

Table 3-5 lists the design specifications for this processor. This system is one of the few real-time hybrid systems in existence, and it achieves this status because the design approach, which separates the pulse compression from the Doppler processing, divides the resolution requirements between two input transducers. Other approaches that perform both tasks in one step are much more difficult to implement because of the lack of suitable high resolution transducers.

Table 3-5 — Design Specifications for
BMDATC Radar Signal Optical Processor

Time-bandwidth product	270,000
Bandwidth	150 MHz
Time resolution	7 nsec
Time elements	900
Doppler resolution	530 Hz
Doppler elements	300
Reference change rate	30/sec

3.4.3 Prototype Hybrid Processor

For the sake of completeness, a demonstration hybrid system that has been assembled by workers at Carnegie-Mellon University must be mentioned.[13] Unlike the Ampex-BMDATC processor, the CM system was not designed to fulfill a particular processing role. Instead, the system was assembled to demonstrate the major features of a hybrid system.

The basic structure of the CM system is shown in Fig. 3-10. The three most important pieces of equipment are the electrically addressed light modulator (EALM), the output signal transducers (Vidicons), and the mini-computer that controls the operation of the entire system.* The optical components that define what operations are performed with this hybrid system are adaptable, and this system has been configured to perform matched filtering on text, Doppler processing of linear chirp and stepped FM radar signals, and beamforming for linear and planar phased array radars.

One of the important hybrid functions that was demonstrated with this system was signal thresholding and fixed noise removal in the output correlation plane. This was possible only because the minicomputer was able to examine each and every output frame.

---

*Both the Fourier transform and correlation planes of the system are interfaced to the PDP 11/15 through the vidicons and a special purpose interface. In certain applications, the PDP has been used to control the input to the EALM. The EALM in this system was an electron-beam-scanned $KD_2 PO_4$ crystal which has a 10^6 space-bandwidth product and a 30-Hz cycle rate.

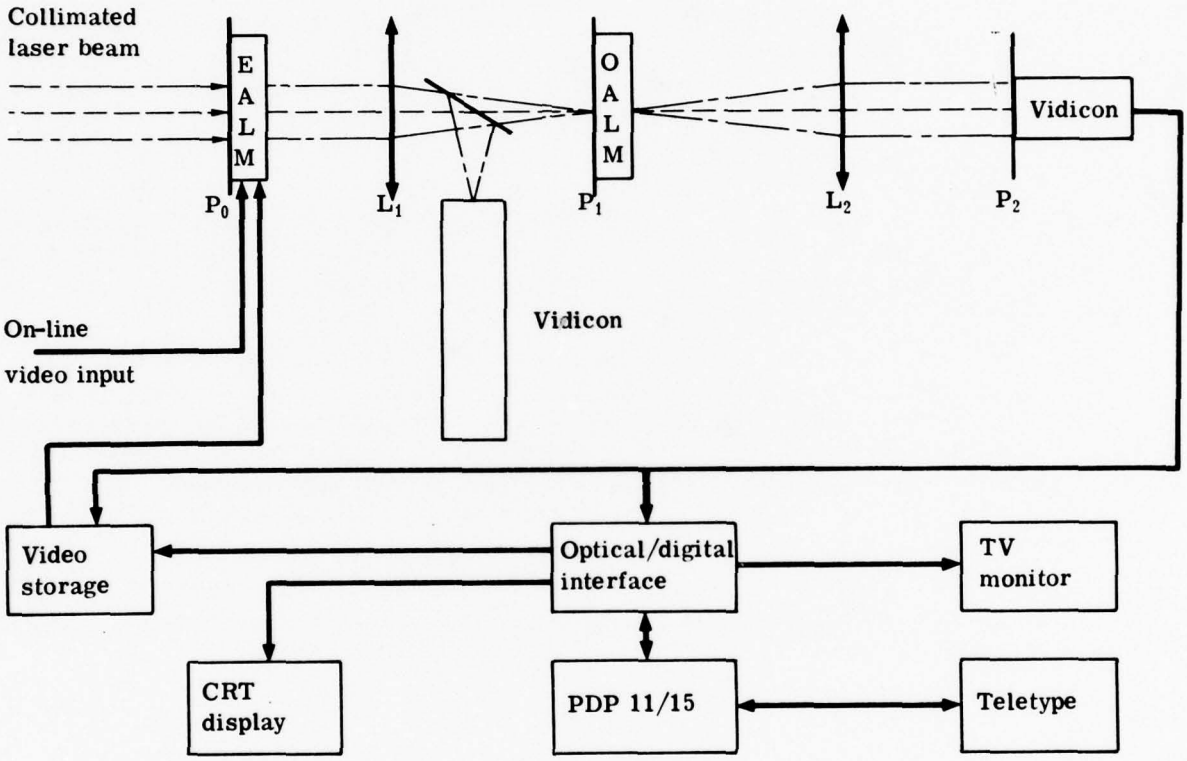

Fig. 3-10 — Block diagram of a hybrid optical/digital processor

3.5 REFERENCES

1. Pernick, B., et al., Appl. Opt., 17:21 (1978).
2. Lukes, G., Proceedings of the S.P.I.E., 45:265 (1974).
3. Lukes, G., Proceedings of the S.P.I.E., 117:89 (1977).
4. Wertheimer, A., and Wilcock, W.L., Appl. Opt., 15:1616 (1976).
5. Hecht, D.L., Opt. Eng., 16:461 (1977).
6. Sprague, R., et al., Optical Signal Processing for Terminal Defense Radars, Final Report, Contract DASG60-75-C-0103, p2-7. (1976).
7. Thomas, C.E., Appl. Opt., 5: 1782 (1966).
8. Von der Ohe, W., Proceedings of the S.P.I.E., 128:210 (1977).
9. Grumet, A., et al., Optical Matched Filter Image Correlator, Final Report, Contract DAAK 02-74-C-0275 (1975).
10. Iwasa, S., Appl. Opt., 15:1418 (1976).
11. Preston, K., Task Reports, Optics in Radar System, P. Poulson ed., Proceedings of the S.P.I.E., supplement to Vol. 128, p. 41. (1977).
12. Brown, H.B., and Markevitch, B.V., Proceedings of the S.P.I.E., 128:204 (1977).
13. Casasent, D., and Sterling, W.M., IEEE Trans. on Computers, C-24:348 (1975).

4. HR^3 BASED TARGET IDENTIFICATION SYSTEM CONFIGURATION

4.1 OVERVIEW

The third phase of this study involved the development of a baseline hybrid system design that could be used both to demonstrate the application of hybrid techniques to the HR^3 target identification problem and to provide a framework for parameter tradeoff investigations. In addition, examination of such a baseline system provides insight into appropriate directions for future study. The results of the first two phases of this study are incorporated implicitly in the baseline design.

Fig. 4-1 is a data flow diagram that shows the various major steps required to perform target identification using high range resolution as the primary sensor. Those tasks for which hybrid subsystems are possible have been identified. The basic division of processing tasks has been made along the lines described in Section 2 of this report: hybrid analog systems have been suggested for tasks involving correlation, Fourier transformation, or integration, while digital or electrical systems have been used for data manipulation and interpretation.

Several difficulties that relate to uncertainties in the processing algorithms were encountered in developing this flow diagram. For instance, the block labeled "phase alignment" represents those processes that eliminate the movement of the center of rotation of the target. No single algorithm has been developed that is universally accepted as optimum. Therefore, for the sake of this study, an algorithm that operates only on single epochs is assumed.

Similarly, the lack of a data base at this time makes it impossible to tell if image correlation techniques will prove useful to target identification. A choice between whole image correlation and feature extraction techniques also exists but cannot be made conclusively, because of this lack of data. Again, for the sake of creating a baseline system design, the whole image correlator has been included.

As shown in Fig. 4-1, the processing steps (after the radar receiver has produced a raw return on an appropriate IF carrier) are:

1. Pulse Compression. This is performed optically with an acousto-optic cell imaged onto a reference mask and the zero-order light is detected coherently.

2. Data Buffer and Phase Alignment. Each range sweep is temporarily stored and digitally aligned (range and phase).

3. Raster Recorder. Each compressed pulse is recorded on an optical medium after an artificial carrier has been injected so that phase can be recorded optically. The raster format is one range sweep per line.

4. Optical Fourier Transforms. The raster-recorded data is optically Fourier transformed to generate images that are turned back into electrical signals by the detector.

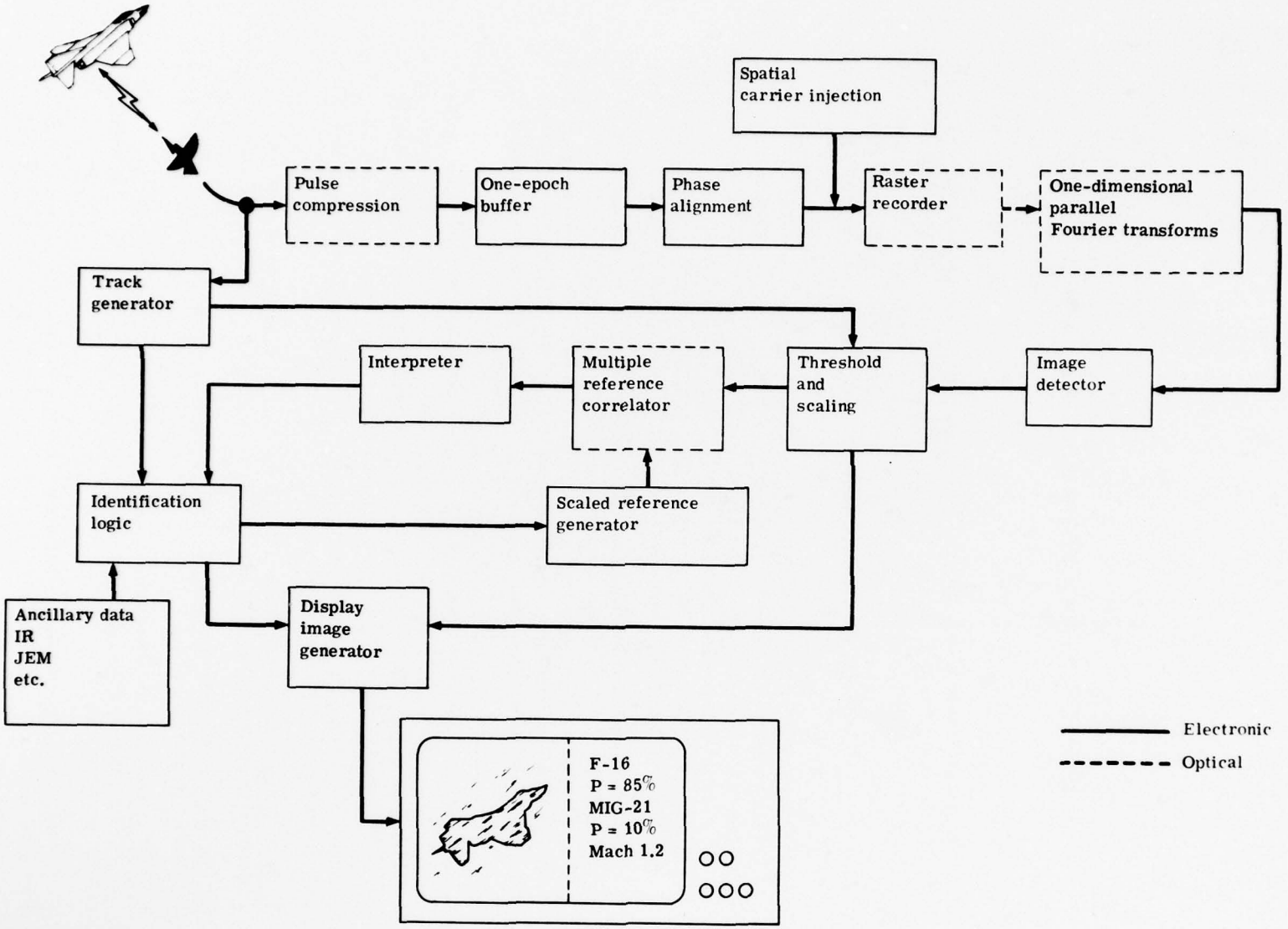

Fig. 4-1 — HR^3 based target identification

5. Thresholding and Scaling. This digital process eliminates the background noise from the image, and uses the tracking data to orient and scale the image to some predetermined values.

6. Multiple Reference Correlation. This optical correlation accepts the scaled and oriented images (electronic-to-optical conversion has taken place) and cross correlates with a reduced set of reference images produced by the memory bank in the scaled reference generator. The size of the reference set is reduced because (1) not all orientations are required and (2) some references have been eliminated by the identification logic. Note that there is an iterative loop here.

7. Interpreter. This is just a detector system that makes threshold decisions on the correlator output.

8. Identification Logic. The heart of the system, identification logic accepts information from the correlator, the track generator, other sensors, and human operators in order to select the most likely identification.

The output from the identification logic is fed into the display system, which consists of a display generator and a terminal. The display generator draws outlines of the aircraft specified by the logic and generates the appropriate alphanumerics. These are combined on the display screen with the image formed by the Fourier transformer (after thresholding and scaling).

All of the processing steps from the raw radar returns up through the thresholding and scaling operation are parts of the signature generator. The multiple reference correlator (with scaled reference generator) and the interpreter form the target classifier, and the identification logic, naturally, is the target identifier.

Working through the system, it is clear that the three stages of processing represent three levels of decreasing information entropy. That is, the processing of the data takes a lot of unorganized data and reduces its volume while increasing its order. As in thermodynamics, reducing the entropy locally requires an input of effort, represented here by the processing systems. Because it is the nature of hybrid processing that the optical subsystems best perform "mindless" tasks at the speed of light while the digital subsystems excel at comparative, logical, and order-forming tasks, it is only natural that the processors that operate on the most disordered information be optical while the processors that operate on the most organized and highest quality data be digital. Thus the identification logic is all digital while the signature generator is mostly optical.

In the sections that follow, the hybrid subsections of the system of Fig. 4-1 will be discussed at greater length.

4.2 MAJOR COMPONENTS

4.2.1 The Pulse Compressor

In the hybrid HR^3 processor, the first opportunity to use an optical subsystem is in the pulse compressor. Because of the large time-bandwidth product required for simultaneous range and cross-range resolution, currently available pulse compression systems are hard pressed to meet the need. Additionally, a real-time pulse compressor is needed to permit the high pulse repetition frequencies required for multiple target tracking. The pulse compression subsystem that is the most likely candidate is similar to the moving window correlator used by Ampex for the BMDATC range-Doppler processor.[1*]

*References are listed in Section 4.4

In the correlator, a Bragg cell is used to create a moving image of the radar signal, which then slides by a fixed reference signal mask. As the image moves past the reference, a lens collects the light passing through the mask and performs a spatial integration of the product signal to generate the correlated output (i.e., compressed pulses) on a detector. The phase of each compressed pulse is conserved in this operation. And, if the detector is illuminated with an appropriately tilted reference beam of light, the compressed pulses will appear with a phase-shifted carrier. The reference beam of light serves as a local oscillator that reintroduces the IF carrier under the compressed pulses.

The advantages of this pulse compressor are its relative simplicity, its use of a Bragg cell as the electrical-to-optical transducers, and its adaptable reference waveform. The major limitations of the system are its time-bandwidth product (limited by the Bragg cell) and the fact that the phase of the compressed pulses are still encoded on a carrier. The first limit is a matter of current research activity because the use of Bragg cells in spectrum analyzers is quite popular.[2] It may be expected that the current practical TBW of 1×10^3 will be increased by an order of magnitude soon. The second limitation is more inherent in the concept of operation. However, as a practical matter, this system simply shifts the phase measurement operation back into the electronic domain where it would have been addressed in any case. This comment is not meant to trivialize the problem, rather it is meant to point out that hybrid techniques can ease some data processing problems but not others.

If the pulse compressor is viewed as part of the processing pipeline, the time delay (which is the length of the pipeline) is just the fill time of the Bragg cell, and the rate at which targets may be processed is unlimited. As discussed in Section 2.5.3, the number of parallel correlators required in the HR^3 system will be determined by the unambiguous range window and not by the correlator.

4.2.2 Phase Alignment Subsystem

The second major operation that must be performed on the compressed pulses is called phase alignment. In essence, this operation is designed to take out the effects of the linear motion of the center of target rotation. Several algorithms have been considered for this subsystem by other firms, and no one algorithm seems ideal. In keeping with the pipeline approach and considering the requirement that the radar will be interrogating several targets in a repeating sequence, it has been deemed desirable that the phase alignment system operate on single pulse return epochs only. That is, phase alignment will be performed on each set of compressed pulses coming out of the correlator individually. The most likely algorithm is the selection of the nearest scattering point as the virtual center of rotation.

To implement this algorithm, the phase of the first pulse out of the correlator is subtracted from the phase of all of the pulses. As discussed in Section 4.2.1, the phase alignment must be performed in conjunction with the measurement of the phase. However, since the alignment algorithm just requires a knowledge of the first and current pulses' phases, a pipeline implementation is quite suitable. Unlike the pulse compressor, the phase alignment subsystem is not real-time and the high bandwidth of the IF carrier on which the phase information is coded may require parallel processing channels to permit pipelining.

Another step that is included in this subsystem is range alignment, an operation that is nothing more than placing the first scatterer in the same range bin for each epoch.

4.2.3 Raster Recorder (Data Storage)

The imaging algorithm requires that many epochs of compressed pulses by stored before a full resolution HR^3 image can be produced. In a digital storage system, the pulse values can be stored in active memory, on tape, or on a disk file. Since the epochs from any one

target are interspersed with the epochs from other targets, the organization of the data in any of these memories can be either sequential (with a library of where all the epochs due to one target are filed) or by target. In any event, a significant processing overhead results when the data is called from memory for the next stage of processing.

An alternative to the digital storage system, a hybrid raster recorder that stores data in analog format on an optical medium, has been considered. Essentially the recorder is a scanning laser beam that is modulated to produce a line of varying density on a piece of film. In order to record complex data such as the compressed pulses, a spatial carrier of the proper phase must be injected under the modulation envelope of each compressed pulse. For the hybrid processing system, this form of data storage has several advantages. These include high density storage, suitability for input to optical Fourier transformer, continuous readability, and capability of direct multiplexing for multiple target storage.

The major reason for using an optical storage medium is, to look ahead one step, the desirability of performing optical Fourier transforms in the next stage of the hybrid processor. The optical storage eliminates the later data conversion. Another important advantage of optical storage is direct read-after-write. Depending on the optical medium used, immediate readout of the stored data is possible. Thus, as radar pulse epochs are stored, it would be possible to optically Fourier transform the partially filled data array. In this manner, an early identification of the target may be possible, based on the low resolution image formed from the incomplete data array.

One difficulty normally associated with optical raster recorders is the lack of a random access capability. In practice this means that radar data from the multiple targets being tracked must be recorded sequentially, thus interspersing the epochs from all the targets. Similarly, upon readout the data generally cannot be selectively collected into arrays before Fourier transforming. However, because of the high storage density of optical media, there are at least two techniques for overcoming this difficulty: spatial multiplexing and frequency multiplexing.

Of the two, the former is more easily understood and will be presented first. Basically, spatial multiplexing on an optical storage medium is nothing more than recording data from different targets side by side down the length of the optical medium. With proper timing of the radar pulse epochs (achieved with first-in, first-out buffers), the raster recorder acts as a serial-to-parallel converter. It takes a series of epochs from different targets and converts them into parallel columns of data. As an example of how the capabilities of current raster recorders would fit this application, the Itek Real-Time Recorder and Display (RTD) will be considered.

The RTD takes a stream of digitized pixels at up to 6 megapixels per second and records them on a metal-on-plastic material by burning small holes of varying size in the metal. Each line of data contains 10,000 pixels of 5 to 6-micrometer size. In the HR^3 application, each radar pulse epoch contains perhaps 200 range bins. If 10 pixels are alloted to each range bin (to permit recording the phase encoded carrier), then five epochs can be recorded on each line of the RTD. Thus five channels (or targets) can be incorporated into the one device. As this data emerges from the recorder, five separate lens systems can be used to perform parallel Fourier transforms on the five channels of data.

The second technique for optical recording is frequency multiplexing. In this technique, each epoch is recorded on a sequential line in the raster, but epochs from different targets have their phases encoded on distinct carrier frequencies. Thus, all the target points on the first target are recorded on the optical medium as little gratings of frequency f_1 (albeit with different phases), the second target's points are little gratings of frequency f_2, and so on. When these

gratings are Fourier transformed, all the target points from the first target are imaged at an off-axis angle proportional to f_1, the second target at an angle proportional to f_2, etc.

As a quick demonstration of this technique, the Itek RTD was used to create two gratings: one grating had frequency f_1 and phase ϕ_1, and the second had frequency f_2 and phase ϕ_2. Thus each grating represented a one-scatter target. When these gratings were optically Fourier transformed, the point images shown in Fig. 4-2 resulted. The two gratings were then interleaved, simulating sequential recording of epochs. The interleaved gratings are shown in Fig. 4-3a and the resulting Fourier transform in Fig. 4-3b.

It should be noted that these recording techniques can be combined to increase further the number of targets that can be recorded simultaneously on one raster recorder.

4.2.4 Optical Fourier Transformer

If it is assumed that the raster recorder described above is used to accumulate the data from the radar targets, then the use of a lens to perform the required Fourier transform is both natural and practical. As a review, the imaging algorithm calls for compressing the returning pulses along the range coordinate to achieve range resolution and Fourier transforming across the sequential epochs to achieve cross-range resolution. Since the pulse compression has been performed by the "front end" of the hybrid processor, the Fourier transform stage of the system actually performs an imaging in the range direction while performing the Fourier transform in the cross-range direction.

Fourier transforming and imaging are the natural operations that can be performed with coherent optical systems. An anamorphic optical system, similar to the SAR processors, can be located at the output side of the raster recorder. As the recorder data scrolls out, it may be illuminated by a beam of laser light. At the image plane of the lens, the radar image will appear instantaneously. This is true pipeline processing, with the only delay being the time required to physically transport the lines of recorded data from the raster recorder to the input plane of the optical system. Because the Fourier transformation process takes place literally at the speed of light, it is possible to perform the transform "continuously," i.e., while the data is in the process of coming out of the raster recorder.

As the first several lines of data enter the optical transformer, a low resolution image will be formed. The resolution will depend linearly on the number of lines in the field of view. Thus, as more lines become available, the image resolution will improve. The images based on the partial data may prove adequate for target identification; in that case, the control computer could release the HR^3 system in order to acquire a new target. In a digital Fourier transform system, this technique would be quite expensive in terms of computing burden, and would probably not be implemented. It should be noted that these partial transforms can be performed because the movement of the data in the input plane has no effect on the intensity of the formed image.

The actual optical layout of the Fourier transformer will depend on the recording technique selected. For example, a spatially multiplexed recording will require identical parallel transforming channels, while a frequency multiplexed system would require a single large aperture system with multiple image planes.

The image formed by this system must be detected in order for the next stage of processing to occur. At the present time, the most likely candidate device is the CCD. Thirty times per second these detectors would send image frames to the next processing stage.

4.2.5 Multiple Reference Correlator

The last major subsystem of the hybrid processor that involves optical techniques is the image correlator, which is used to help identify the target based upon the characteristics of its radar image. The input to this subsystem comes from the threshold and scaling systems

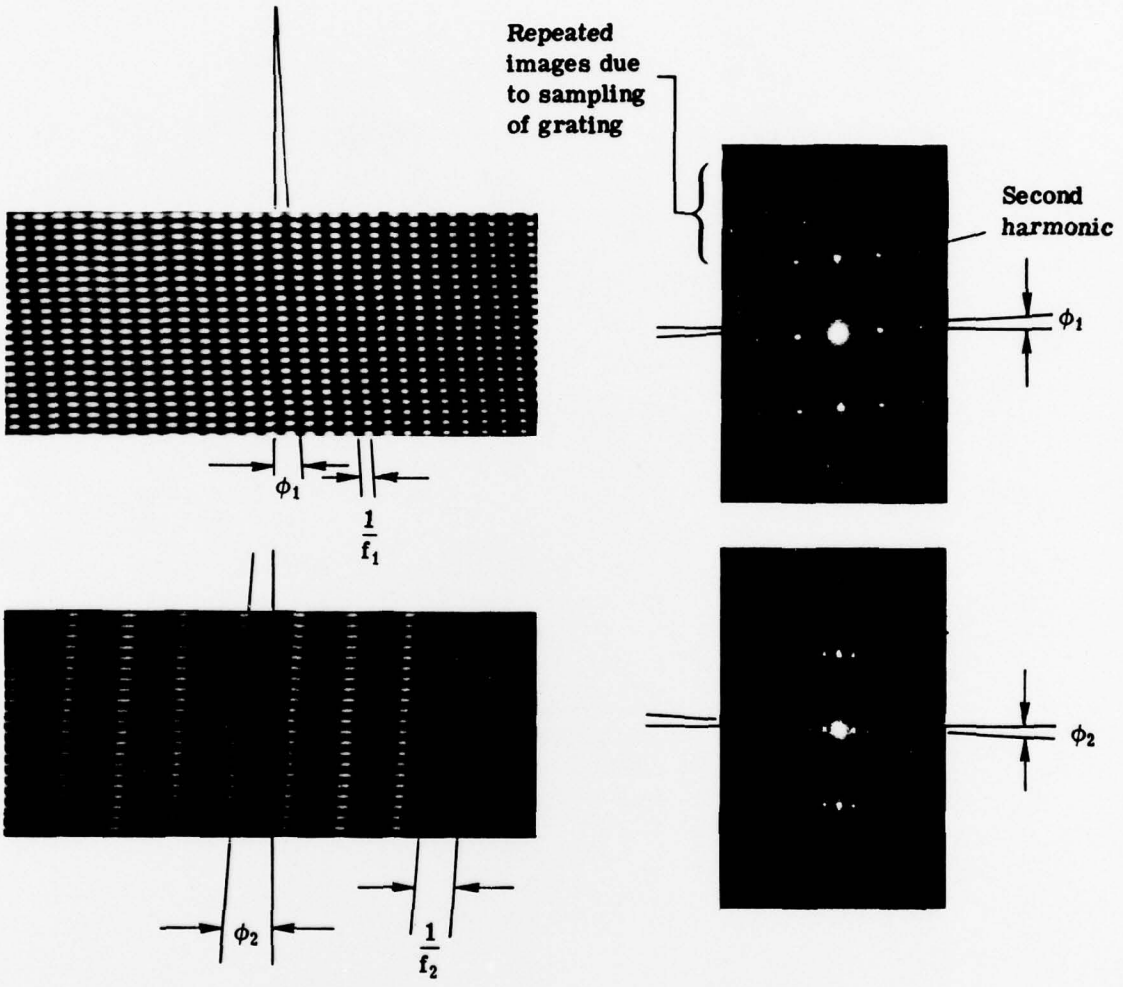

Fig. 4-2 — Non-multiplexed gratings and their transforms

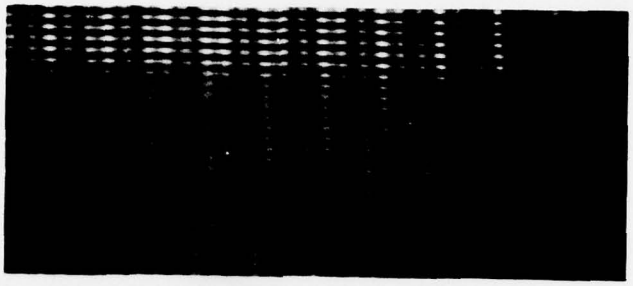

(a) Multiplexed grating

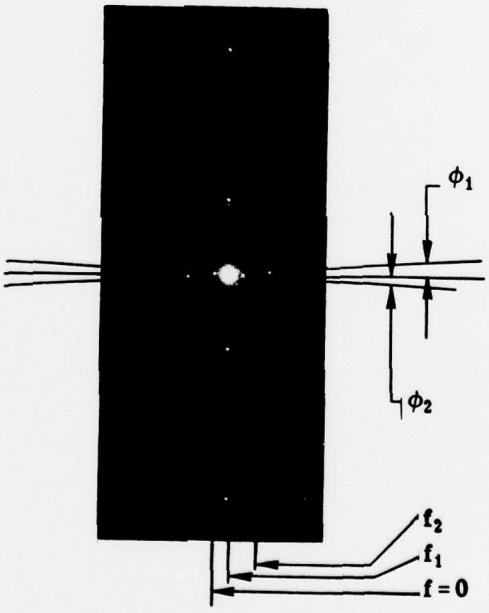

(b) Fourier transform

Fig. 4-3 — Frequency multiplexing demonstration

connected to the output image detectors in the Fourier transformer. The purpose of the threshold and scaling system is to clean up and standardize as far as possible the inputs to this correlator in order to minimize the search time for a recognized target. Some of the operations that might be performed by the scaler are aspect ratio correction, image rotation (e.g., nose toward top of image), and intensity dynamic range compression. These partially standardized images are compared to a set of reference images in the multiple reference correlator.

Several approaches, such as those discussed in Section 3, have been considered for this correlator. These divide naturally into fixed reference correlators (such as the Grumman ground target recognition system) or adaptable reference correlators. The latter type has not been built in a real-time implementation because of the cost and technical difficulties involved. Nevertheless, because of the dimension of the HR^3 target recognition system, such an approach is likely to be required here.

In an adaptable reference correlator, the one unknown image is tested against one or more reference images that have been stored outside the correlator per se. The reference images are changed repeatedly until the best match or template for the unknown image is found. In the HR^3 application the dimensionality of this search is high because of the many possible aspect angles and many possible targets. However, depending on the quality of the auxiliary data that is available, the dimensionality of the search might be reduced to a reasonable size.

The nature of HR^3 images suggests that the best type of correlator for this application is one that utilizes an image plane reference. HR^3 images can be modeled as a finite (and small) set of scattering points in three space. If the reference targets are stored in a digital memory as the set of coordinates of the scatterers, then these scatters can be projected into the expected HR^3 image plane by simple geometry and a single, properly oriented and scaled reference image generated to match with the unknown target image. This image generation technique is similar to that used by SRC to produce target outlines for human template matching.[3] However, this technique will require the development of a modeling technique that can predict radar scattering cross sections based on known visible target features (e.g., photographic data).

The most likely candidate for this image plane correlator is the so-called joint transform correlator.[4] In the JTC, the unknown and reference images are placed side by side in the front focal plane of a lens and illuminated with a plane wave of light. This forms the joint Fourier transform of the two images on a real-time spatial light modulator (SLM) located in the back focal plane of the lens. After the intensity of the transform is stored, the SLM is read out and retransformation performed. Since this is a retransformation of the intensity of the spectrum, the output image is the autocorrelation of the entire input. If the two input images were originally separated (inside edge to inside edge) by the width of the widest input, then the output autocorrelation may be partitioned into three distinct regions: one region in which the two inputs' autocorrelations appear and two regions in which the cross correlation of the left and right images appear.

For the HR^3 application, an SLM would be utilized in the front focal plane of the lens as well as in the back focal plane. The unknown target image from the threshold and scaler would be combined with a test reference image from the digital memory to form a single side-by-side image. This image would be recorded on the SLM with a scanning beam. The fastest scanning rates could be achieved with a random access scanner because the HR^3 images tend to be collections of spots on a blank background. After the side-by-side image is recorded on the SLM, the correlation is performed and a detector in the output plane measures the strength of the correlation spot. The output detector is likely to be a small array (5×5) to account for small positioning errors in the input images. The correlation cycle is repeated with new reference images until enough information has been gained to identify the target.

The output of the correlator is sent to the identification logic through a digital interpreter, which performs such tasks as normalization and thresholding. The identification logic feeds information back to the correlator by commanding the list of reference targets to be tried. This list is adjusted by decisions made on the basis of information from all sources. Thus, if the speed of the target based on tracking data eliminates cargo transports, then no reference images of that class target will be used in the correlation cycle.

The remaining subsystems in the HR^3 target identification system are purely digital. The major component is the identification logic. At the present time, no single fusion algorithm has been identified that will optimally recognize targets, but without question the selected algorithm will be best suited to a digital implementation.

4.3 CRITICAL TECHNOLOGIES AND COST ESTIMATES

As a practical matter, the implementation of a hybrid processing system similar to the one described above will require continued technology developments in several areas. Also, the implementation will require adequate funding.

The technologies that are most critical to the HR^3 processing system are spatial light modulators, acousto-optic Bragg cells, and optical storage media and technologies.

4.3.1 Spatial Light Modulators

The real-time joint transform correlator requires the use of two spatial light modulators (SLM): one in the input plane and one in the transform plane. The resolution and space-bandwidth product of the input plane is determined by the requirement of storing two images side by side. Since there are only about 300 resolution points across an HR^3 image, a space bandwidth product of about $1{,}000 \times 500 = 5 \times 10^5$ would be adequate to store two side-by-side images with appropriate spacing. For most SLM's a 25-millimeter dimension is standard, yielding a 40-cycle-per-millimeter resolution requirement. The input plane device must also be flat to about 1/2 wave in order to preserve its coherent optical processing capabilities. The Fourier plane device must be capable of similar resolution and space-bandwidth product performance and, in addition, it must be sensitive to the readout light from the first SLM.

At the present time, the choice of SLM's is effectively limited to the Itek PROM, the Hughes LCLV (Liquid Crystal Light Valve), and the General Electric light valve. KDP Pockels devices have been constructed, but they are not commercially available. None of these devices is wholly suitable for both the image and Fourier plane devices, and the 40-cycle-per-millimeter requirement is beyond the comfortable limit for all of them. The standard operating rate for the devices is less than or equal to 30 Hz, a limit that may produce a processing bottleneck. The G.E. and Hughes devices are limited by their decay characteristics, but the PROM, which is flash erased, should be operable up the 1 to 2-kHz range with appropriate electronics.

Considering the possibilities, the best devices for the real-time joint transform correlator would be a Hughes device in the input plane (addressed from the digital subsystems via a crt) and an Itek PROM in the Fourier plane. Note that the LCLV may be read out nondestructively with the blue light to which the PROM is sensitive.

4.3.2 Acousto-Optic Bragg Cells

The A-O Bragg cell is used as the electrical-to-optical converter in the pulse compression processor. These devices operate by the propagation of sound waves through crystaline material. Light passing through the crystal at the same time is diffracted because it interacts with the layers of compressed and rarified crystal. Because the layers are thick (in optical terms), the diffraction efficiency of the cells is angularly sensitive (i.e., Bragg diffraction). Additionally,

the crystaline materials are acoustically dispersive (different frequencies travel at different velocities) and have high absorption at high acoustic frequencies. These three effects (angular sensitivity, dispersion, absorption) combine to limit the time-bandwidth products of the A-O cell. If the center frequency is raised to reduce the fractional bandwidth (and the dispersive effect), then the useful length of the cell (i.e., the length of the signal) is also reduced because of the high absorption.

Current practical A-O cells have a time-bandwidth product of 1,000 to 2,000. Continuing research into new materials and transducer designs may increase this by an order of magnitude. Also, Itek is pursuing a related area of research, optical diffraction from surface acoustic waves, that may overcome many of the Bragg cell difficulties.

4.3.3 Optical Storage Media and Technologies

One of the more demanding requirements in the HR^3 program is the need to build up in storage and to transfer large blocks of data. In the strawman system, an optical raster recorder is suggested. The utility of an optical storage system is heavily dependent on the development both of recording techniques that make up for the nonrandom-access nature of optical storage and of an optical storage medium that has the properties of rapid, nonchemical development and coherent optical compatibility. These two properties are essential in an optical storage medium since the lack of the former would be too burdensome and the lack of the latter would remove the raison d'etre for an optical storage system (i.e., direct optical Fourier transformation from the storage medium).

Several possible media exist. Itek has been investigating the class of materials known as metal on plastic. MOP materials are recorded on by ablating small, 5-micrometer, holes in the metal with a focused beam of light. Generally, a laser is used, but Itek has been investigating solid-state sources for more efficient system designs. While MOP certainly satisfies the dry, instant processing requirements for the HR^3 optical storage medium, its coherent optical properties have not yet been investigated. Potential difficulties exist because of diffraction effects off the sampled signal structure or because of phase variations in the plastic support base. These are questions that await an answer.

4.3.4 Cost Estimate

If it is possible to assume that these technology questions can be answered, then it is legitimate to speculate as to the cost of the HR^3 hybrid processor. The fairest cost estimate would be broken down into development costs (how much does the first system cost?) and production costs (how much for the next 499 systems?). Unfortunately, virtually all hybrid systems built to date have been at the development level, so the effects of "economics of scale" have not been observed. Nevertheless, costs for certain portions of the hybrid processor may be estimated. For example, the Ampex-BMDATC radar processor cost was on the order of $1 million dollars. This breadboard processor included a pulse compression system similar to that suggested for HR^3 processing, two spatial light modulators, and a one-dimensional Fourier transform system similar to that required for HR^3 image generation. This processor did not include a recorder-optical storage system, but it did include a low power raster recorder. The cost of the recorder-storage system may be estimated from the Itek RTD. The RTD cost is estimated to be $750,000 dollars. Both the radar processor and RTD costs include significant design and development costs that could be amortized over many units if they were ever built. Based on these costs, and considering that the HR^3 processor will require the development of a real-time image correlator, a best guess would place the electro-optical costs of the HR^3 processor at $2 to $3 million for the first unit. Digital and electronic components are required to perform phase detection and alignment, spatial carrier frequency injection, thresholding and scaling, processor control, and target identification. The costs of these systems are hard to

define because so much effort in the way of technology development remains. However, it is difficult to imagine the cost being less than $2 million, and twice that figure would not be difficult to consider. Thus, to put a working HR^3 processor on line today would cost anywhere from $4 to $7 million.

4.4 REFERENCES

1. Brown, H.B., and Markevitch, B.V., Proceedings of the S.P.I.E., 128: 204 (1977).
2. "Bragg Cells Spur Interest in Analog Processing for Surveillance Radars," in Electronic Warfare/Defense Electronics, Vol. 10, No. 4, p. 60 (1978).
3. Herman, R.L., et al., "Aircraft Identification by Wideband Radar Imaging," Final Technical Report, Contract F30602-76-C-0098 (1977).
4. Rau, J.E., J. Opt. Soc. Am., 56: 1490 (1966).

5. SUMMARY AND CONCLUSIONS

Itek Corporation has performed a three-part study for the Rome Air Development Center that addresses the use of hybrid optical/electronic processing techniques for high range resolution imaging radar systems in particular and identification friend or foe systems in general. The first part of the study was an investigation of the processing requirements of the HR^3 system. An analysis of the HR^3 imaging processes was performed utilizing an inverse scattering approach. Using the results of this analysis, parametric evaluations were performed that related processor capabilities such as pulse repetition frequency, data storage capacity, and number of parallel processing channels to the basic system operating parameters such as cross-range resolution, target density, target range, and target velocity.

The second part of this study included a survey of hybrid processing systems that have already been assembled. This survey covered illustrative examples of the different types of hybrid processors, including power spectrum analyzers, Fourier transform filtering systems, and synthetic aperture radar processors. Of all the systems studied, only one approached the idealized hybrid processor in which a constant interaction between the optical and electronic subsections was possible. This one system was a laboratory breadboard and not an everyday, working, packaged processor. In addition, except for the power spectrum analyzers, most of the systems studied could not even be classified as real-time processors. A fundamental cost/technology gap exists between the processor concepts and the experimental implementations. This gap will be closed only when there are improvements in the electrical-to-optical transducer technology. Until that time, hybrid processors will need careful design to achieve high performance, real-time operation with today's transducers.

The third part of this study developed a strawman hybrid processor for HR^3 image generation. In keeping with hybrid design philosophy, the system included optical subsystems for pulse compression (i.e., correlation), mass storage, Fourier transformation, and image correlation and electrical subsystems for phase alignment (i.e., revaluing), intensity thresholding, image scaling, and logical analysis of data. A pipeline approach was utilized to minimize the processing time and, because of the natural flow of the data through the subsystems and the high data rate of hybrid systems, most potential processing bottlenecks were eliminated. As an example, the use of an optical storage medium to hold the radar returns during the integration time permitted direct entry of the returns into the Fourier transformer without the processing overhead normally associated with data transfer.

Several conclusions may be drawn from the results of this study. First, the HR^3 image processing algorithm generates such tremendous data burdens that there is a particularly strong need for the high throughput rates of hybrid techniques in the "front end" portions of the processor. In the later sections of the processor, the data has to be reduced and refined so that the problem becomes one of performing higher level processes on fewer data bits.

Second, there already exist hybrid systems that match or nearly match some of the processing tasks that occur in HR^3 imaging. Specifically, hybrid pulse compressors and one-dimensional real-time Fourier transformers are very well suited to the tasks and data rates that exist in the HR^3 processing chain. A second group of hybrid systems exist that might have application in the HR^3 processor, but on which more development effort will be required. These systems include the image correlator and the optical data buffer. A third group of tasks within the HR^3 processor seem unsuited to hybrid techniques. These include those tasks that require logical operations or numerical comparisons.

A third conclusion that may be drawn from this study is that there exists a significant need for continuing research efforts, in terms of both the hybrid systems as applied to the HR^3 application and the HR^3 processing algorithms themselves. The two areas of HR^3 processing where this need is most evident are in phase alignment and in image identification. For the sake of the current study, the assumptions were made that the single-epoch phase alignment algorithm could be used and that sufficient target identification information would be retained in an HR^3 image so that correlation with fixed references would be a useful technique. The validity of the first assumption must be tested analytically while that of the second will require the acquisition of a meaningfully large data base for testing.

Within the framework of advancing the understanding of the application of hybrid techniques to the HR^3 problem, Itek can recommend several courses of action for the near term:

1. A demonstration of HR^3 image generation via a one-dimensional optical Fourier transformer. The data, arrays of compressed pulses with phase modulated carriers, would be prepared off-line and inserted into an anamorphic optical system for processing. Data recording techniques such as frequency and spatial multiplexing could be evaluated. The coherent optical properties of various real-time media (e.g., metal on plastic) could also be determined during this program.

2. The development of a high speed digital-to-optical converter. The primary task in this program would be the development of the spatial carrier insertion system. This system would be the converter that changes the digital phase value into a properly phased grating for recording on optical media.

3. A study of the application of image or feature correlation to HR^3 image identification. This study would require some form of data base upon which testing could be performed. The study could be implemented through either digital simulation or off-line optical correlation. The digital simulation would provide greater flexibility for testing correlation sensitivity to parametric variations, but the optical correlation approach would save the expense of digital processing of large arrays and would test the validity of the optical implementation.

4. The fabrication of a real-time optical correlator. Of all the hybrid building blocks in the strawman system, the correlator appears to require the most development at this time. Since the correlator is the key device in reducing human intervention in the identification process, it is important that this technology be brought up to its highest level as soon as possible. The suggested program would be to develop a joint transform correlator in which the two input images are controlled by a dedicated digital system and in which the output signal is analyzed by the digital system.

Appendix
AMBIGUITY FUNCTION FOR RADAR IMAGING

In this appendix we derive the expressions used for the ambiguity function in Section 2. The ambiguity function is defined by

$$\chi(R'-R) = \int_{-\infty}^{\infty} f\{t - 2[R'(t) - R(t)]/c\} f^*(t)\, dt \tag{1}$$

where f(t) is given by (see Section 2, Eq. 5)

$$f(t) = \sum_{n=-N/2}^{N/2} g(t - n\tau) \exp[i\omega_0 (t - n\tau)] \tag{2}$$

$R'(t)$ is the distance from the radar to an integration point $\underline{r}'$ on the aircraft as shown in Fig. 2-2.

As can be seen from Fig. 2-2, at $t = t_0$, $\underline{R}'(t)$ is given by

$$\underline{R}'(t_0) = \underline{R}_0(t_0) + \underline{r} \tag{3}$$

Since the aircraft is rotating with constant angular velocity $\underline{\Omega}$ about the point $\underline{R}_0(t)$, Eq. 3 is replaced by

$$\underline{R}'(t) = \underline{R}_0(t) + \underline{r} + (t - t_0)\, \underline{\Omega} \times \underline{r} \tag{4}$$

at other times. The magnitude squared of $\underline{R}'(t)$ is therefore given by

$$\begin{aligned} R'^2(t) = R_0^2(t) &+ 2\underline{R}_0(t) \cdot \underline{r} + 2(t - t_0)\underline{R}_0(t) \cdot (\underline{\Omega} \times \underline{r}) + r^2 \\ &+ 2(t - t_0)\underline{r} \cdot (\underline{\Omega} \times r) + (t - t_0)^2 |\underline{\Omega} \times \underline{r}|^2 \end{aligned} \tag{5}$$

Since $R_0 >> r$, Eq. 5 can be approximated to obtain

$$R'(t) = R_0(t) + [\underline{R}_0(t) \cdot \underline{r} + (t - t_0)\underline{R}_0(t) \cdot (\underline{\Omega} \times \underline{r})]/R_0(t) \tag{6}$$

With the Cartesian coordinate system shown in Fig. 2-2, the scalar products in Eq. 6 are given by

$$\underline{R}_0(t) \cdot \underline{r} \cong R_0(t)\, x' \tag{7}$$

$$\underline{R}_0(t) \cdot (\underline{\Omega} \times \underline{r}) \cong R_0 \Omega_e\, y' \tag{8}$$

as long as the aircraft rotates only a few degrees during the period of interest. Hence, Eq. 6 becomes

$$R'(t) \cong R_0(t) + x' + (t - t_0)\,\Omega_e\, y' \tag{9}$$

which is the result quoted in Eq. 6.

In analogy with Eq. 9, R (t) is set equal to

$$R(t) = R_0(t) + x + (t - t_0)\,\Omega_e\, y \tag{10}$$

and Eq. 2, Eq. 9, and Eq. 10 are substituted into Eq. 1 to obtain

$$\begin{aligned}\chi(R' - R) = \int_{-\infty}^{\infty} & \sum_{n=-N/2}^{N/2} g\{t - 2[R'(t) - R(t)]/c - n\tau\} \\ & \times \exp i\omega_0\{t - n\tau - 2[R'(t) - R(t)]/c\} \\ & \times \sum_{n=-N/2}^{N/2} g^*(t - n\tau) \exp -i\omega_0(t - n\tau)\, dt\end{aligned} \tag{11}$$

Since the pulses do not overlap, Eq. 11 becomes

$$\begin{aligned}\chi(R' - R) = \int_{-\infty}^{\infty} & \sum_{n=-N/2}^{N/2} g\{t - 2[(x' - x) + (t - t_0)\,\Omega_e\,(y' - y)]/c - n\tau\} g^*(t - n\tau) \\ & \times \exp\{-i\omega_0 2[(x' - x) + (t - t_0)\,\Omega_e\,(y' - y)]/c\}\, dt\end{aligned} \tag{12}$$

Assume that $(t - t_0)\,\Omega_e\,(y' - y)$ is negligible in the argument of g in Eq. 12 and that it maintains a constant value

$$(t_n - t_0)\,\Omega_e\,(y' - y)$$

during the duration of the n-th pulse where

$$t_n = 2(x' - x)/c + n\tau \tag{13}$$

is the time at which the center of the pulse passes the point (x,y). Then, it follows from Eq. 12 that

$$\begin{aligned}|\chi(R' - R)| \cong & \int_{-\infty}^{\infty} g[t - 2(x' - x)/c]\, g^*(t)\, dt \\ & \sum_{n=-N/2}^{N/2} \times \exp -i\omega_0 2n\tau\,\Omega_e\,(y' - y)/c\end{aligned} \tag{14}$$

which is the result used in Eq. 8.